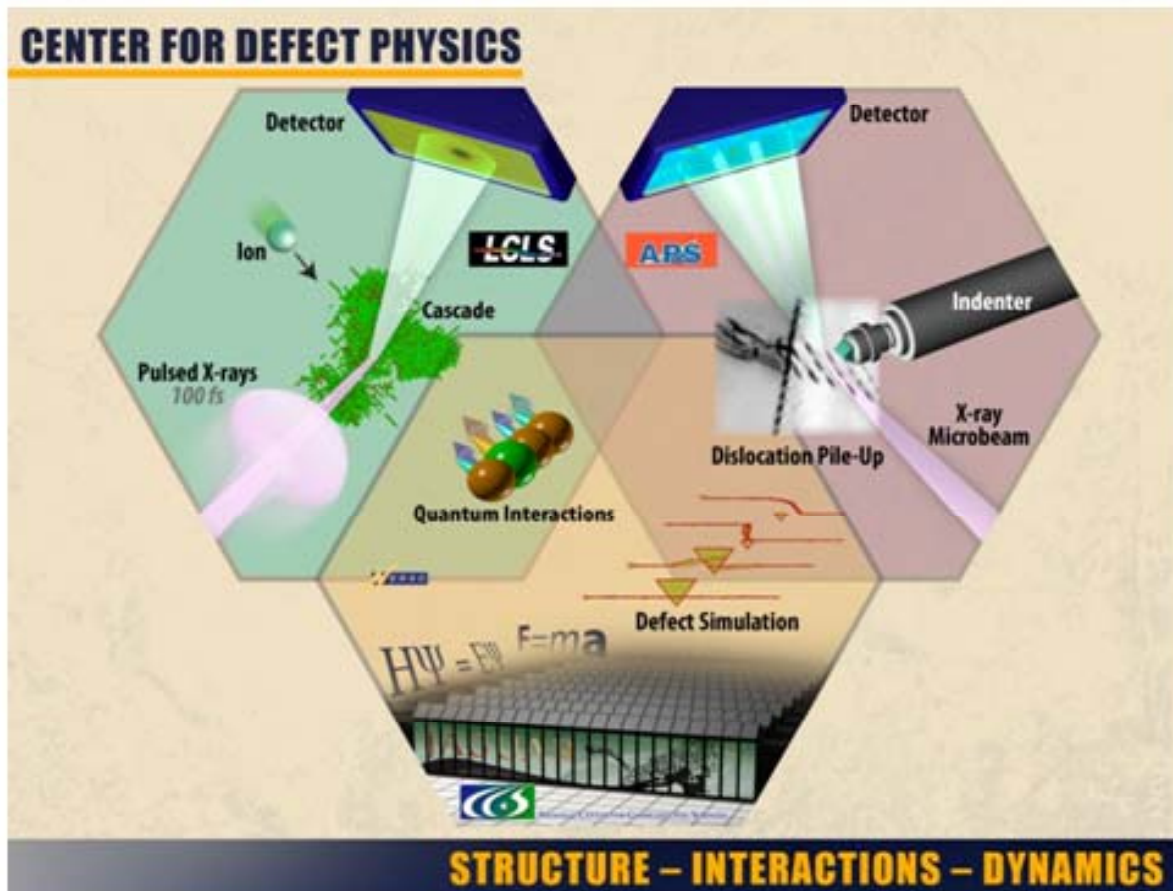


Mechanisms of microstructure evolution under irradiation: defect diffusion, aggregation and interactions.



Yuri Osetsky
Roger Stoller
Stanislav Golubov

Materials Science and
Technology Division,
ORNL

CDP SUMMER SCHOOL
INL

Atomic level Response of Materials to Irradiation

Outline:

1. Nature of radiation damage and effects.
2. Introduction to lattice defects and their properties:
 - Vacancies and clusters
 - Self-interstitial atoms and their clusters
 - Secondary phases
3. Defects mobility and diffusion properties
 - Point defect diffusion
 - Cluster motion
 - Interactions between defects
4. Defects formed in primary damage and damage evolution.
5. Radiation damage as microstructure evolution
6. General formulation of microstructure evolution problem
7. Methods of microstructure evolution modeling:
 - Rate theory
 - Mean field approximation
 - Kinetic Monte Carlo
8. Conclusions and links between scales

The phenomenon of radiation damage

Damage of materials due to irradiation with energetic particles, Radiation Damage, is a very specific phenomenon that is characterized with the following important features:

1. Continuous production of lattice defects due to collisions at primary damage stage and, therefore, continuous increase of the material energy.
2. Motion (diffusion) of radiation induced defects governs microstructure evolution under conditions far beyond the thermodynamic equilibrium that cause enhanced diffusion (Radiation Enhanced Diffusion), changes in phase stability and formation of new high-energy microstructures such as defect clusters, secondary phases, dislocations and dislocation loops, etc.
3. Accumulation of radiation damage puts material into a highly non-equilibrium state and the processes occurred cannot be considered from thermodynamic equilibrium criteria.

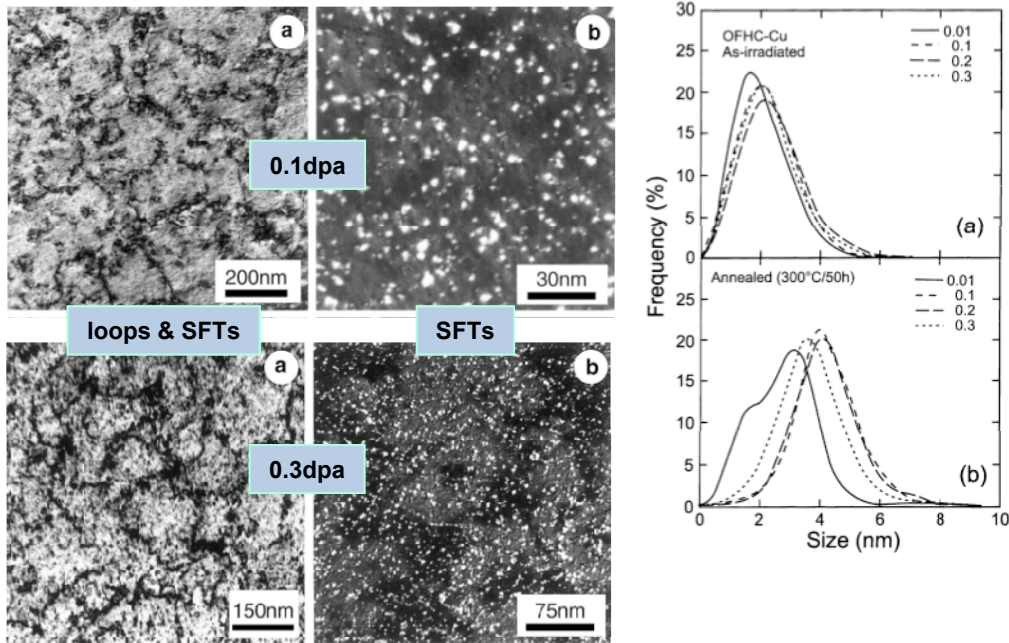
The phenomenon of radiation damage

All above makes theoretical study of Radiation Damage to be a specific area of solid state physics where many operating mechanisms do not exist under equilibrium conditions.

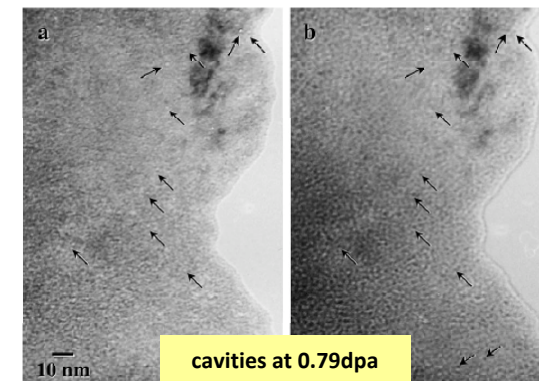
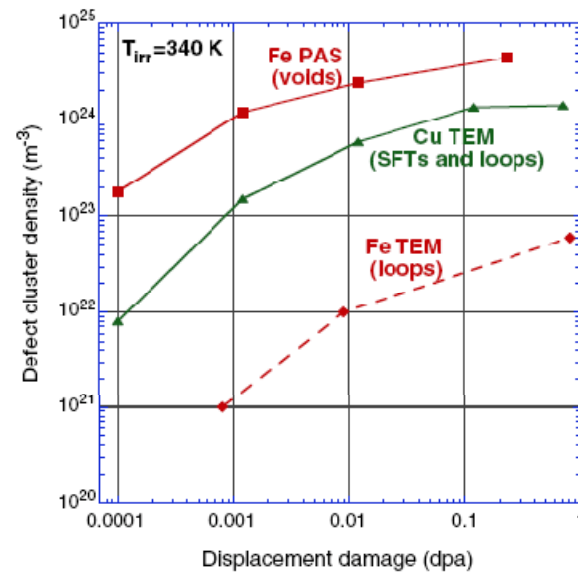
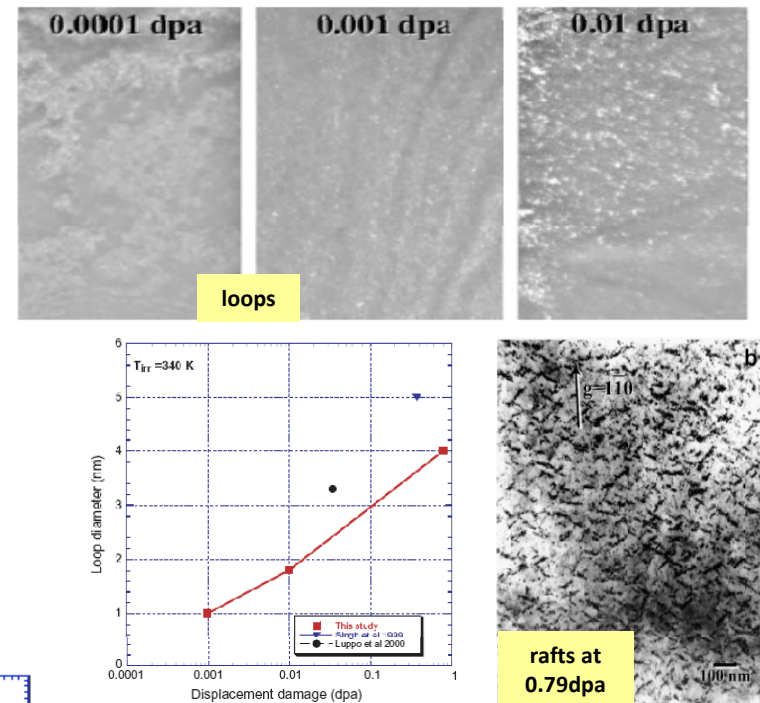
Here we will consider just some basic mechanisms and defect properties that play important role in the process of radiation damage of materials.

Motivation: effect of irradiation microstructure on mechanical properties

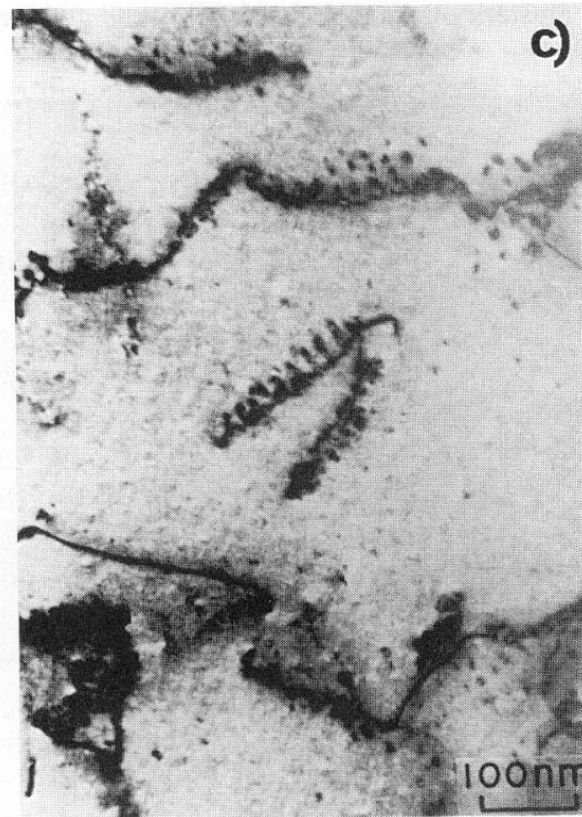
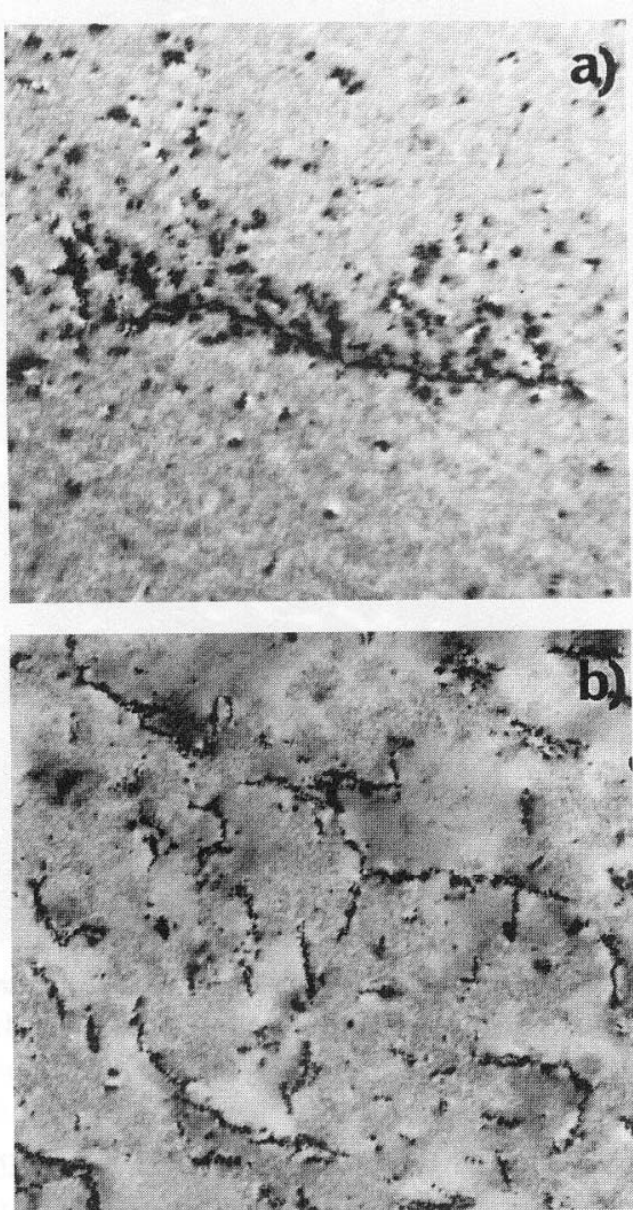
Cu, n-irradiated at 100°C (Singh et al. JNM 2001)



Fe, n-irradiated at 60°C (Zinkle & Singh JNM 2006)



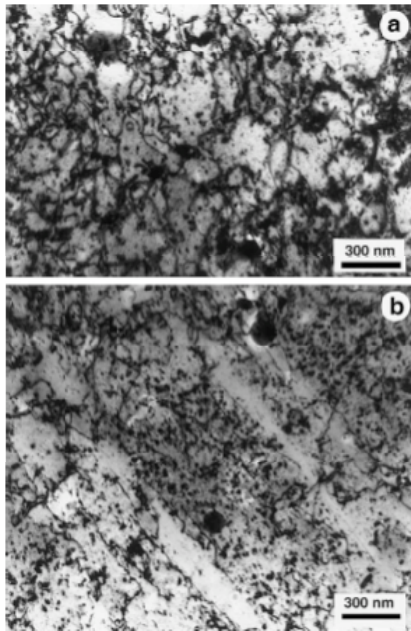
Motivation: effect of irradiation microstructure on mechanical properties



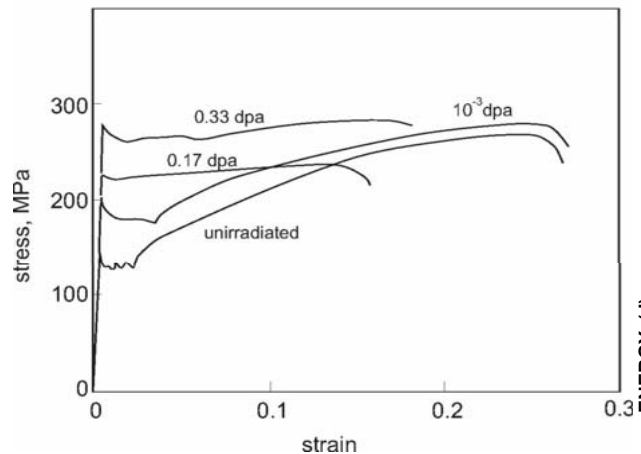
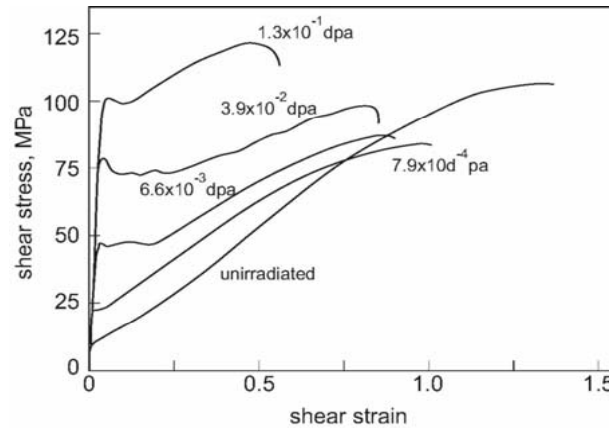
Decoration & rafts: Mo [n]
- Singh & Evans (1997)
- Yamakawa & Shimomura (1998)

Motivation: effect of irradiation microstructure on mechanical properties

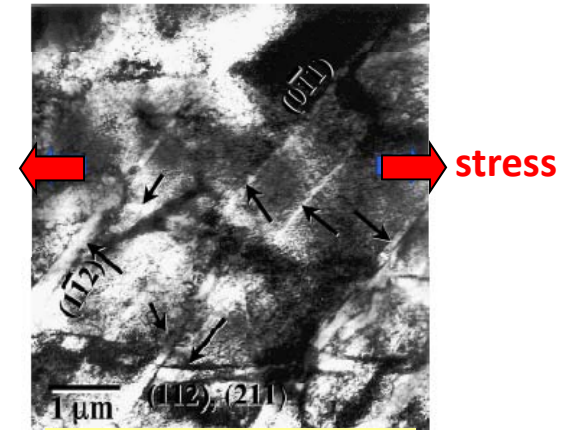
- dislocations under stress move through field of irradiation-induced obstacles
 - dislocation loops, SFTs, point defect clusters, voids, precipitates, etc.



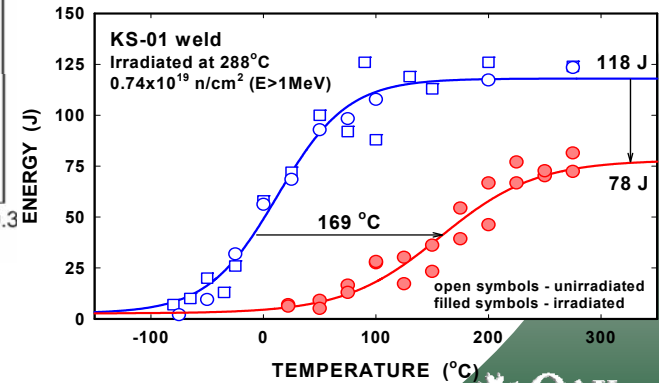
Deformed Cu, n-irrad. 0.01 dpa
 (a) homogeneous, (b) localised
 (Singh et al. JNM 2001)



(a) Single xtal Cu (p⁺-irrad.)
 (b) Polycrystal Fe (n-irrad.)
 - Victoria et al. JNM 2000

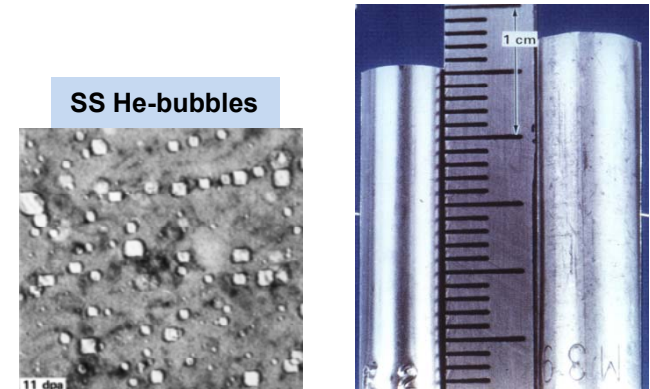


Deformed Fe, n-irrad. 0.4 dpa
 (Zinkle & Singh JNM 2006)



Some effect of radiation damage

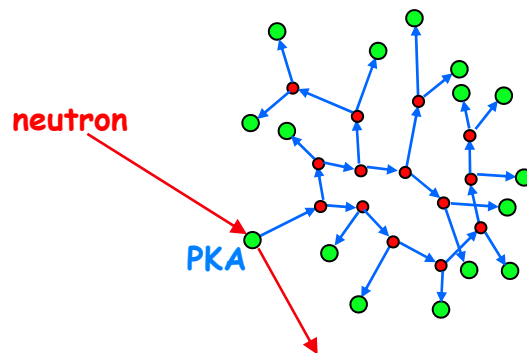
- formation and growth of defect clusters and dislocation loops \ **matrix hardening**
- radiation induced and enhanced diffusion leads to:
 - change in **phase stability**
 - segregation \ **grain boundary embrittlement**
 - precipitation \ **precipitate hardening**
- formation and growth of voids and gas bubbles \ **swelling**
- anisotropic diffusion \ **radiation growth**
- stress induced diffusion \ **creep**



20%CW 316 steel irradiated at T=523C $1.5 \times 10^{23} \text{n/cm}^2$

n-irradiation

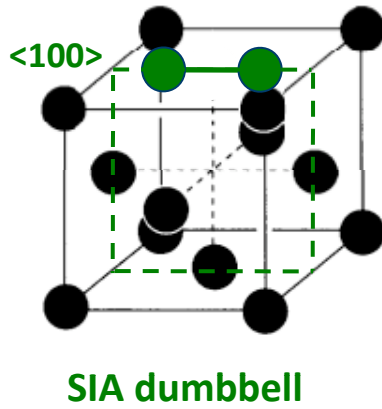
\ defect production ('primary damage') in displacement cascades:



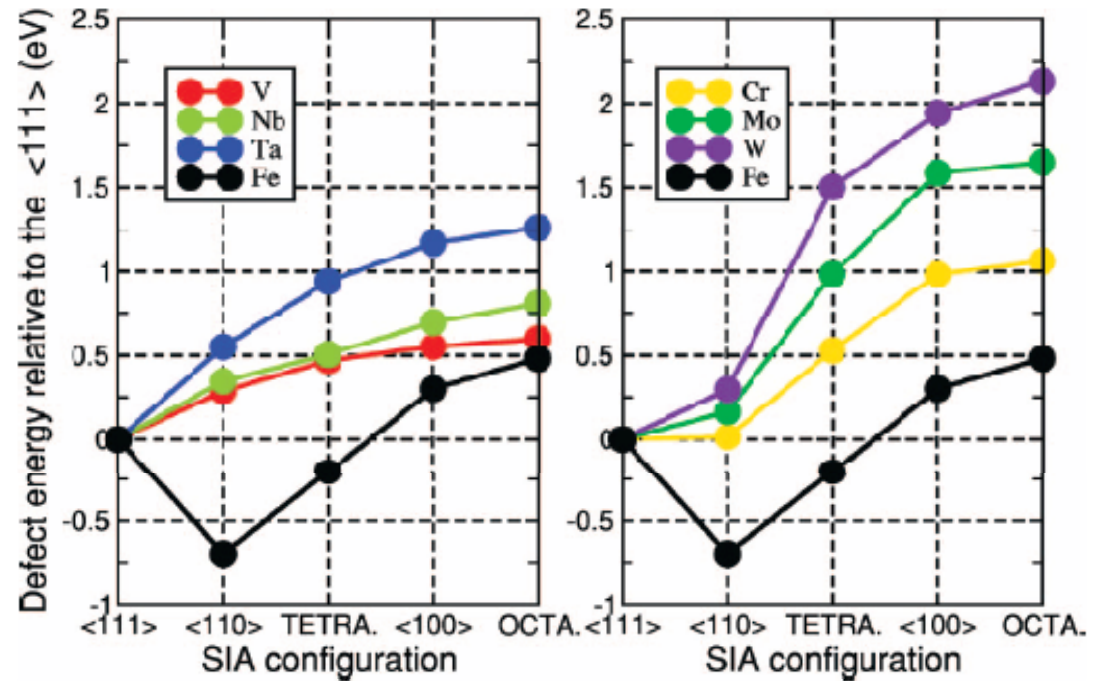
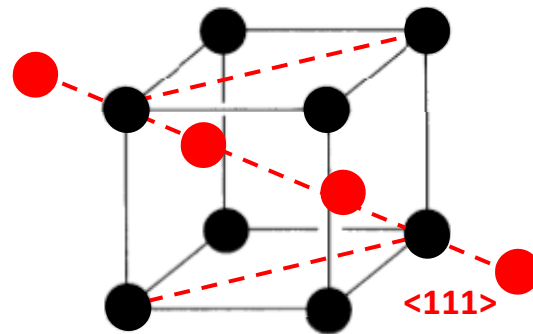
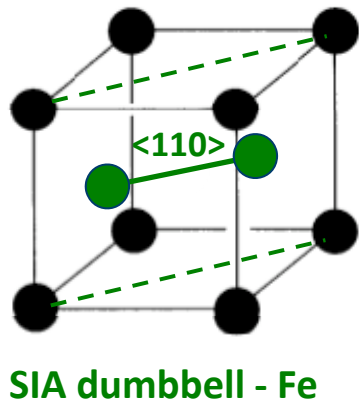
- \ single vacancies and self-interstitial atoms (SIAs)
- + clusters of SIAs (= small dislocation loops - may be glissile)
- + clusters of vacancies (dislocation loops in some cases)

Self-interstitial atoms (SIAs)

FCC



BCC



Nguyen-Manh, Horsfield, Dudarev, Phys Rev B (2006)

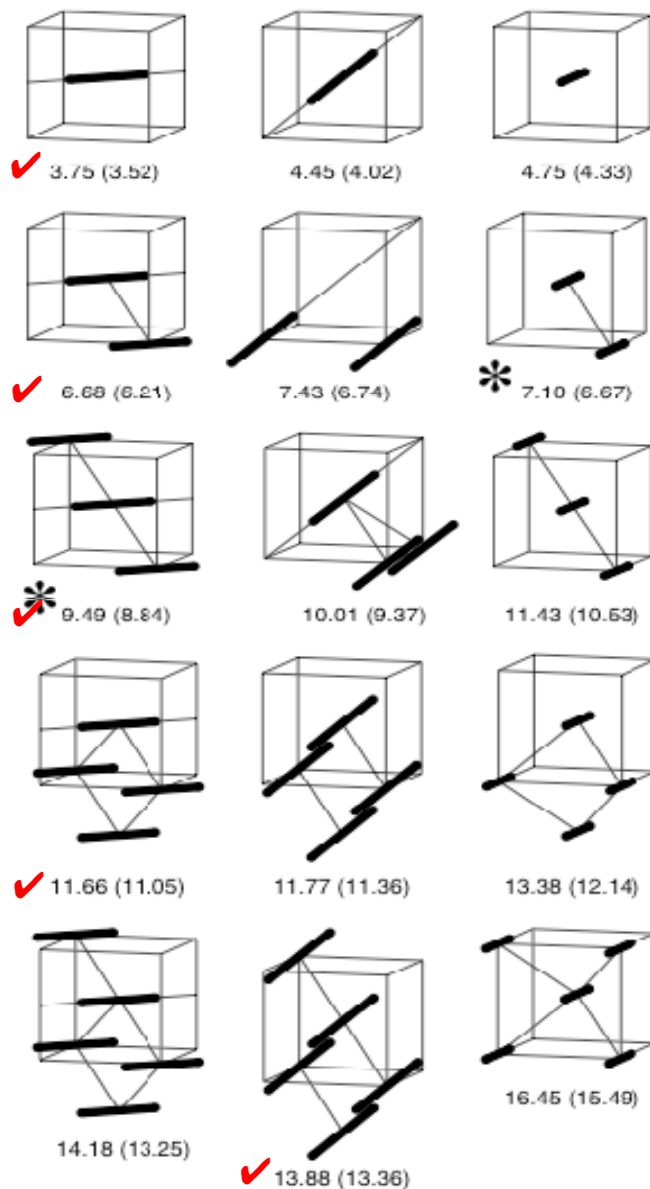


Fig. 4. Schematic representation of the arrangements of the dumbbells with lowest energy in ab initio calculations for the $\langle 110 \rangle$, $\langle 111 \rangle$ and $\langle 100 \rangle$ orientations for interstitial clusters up to I_5 . The ab initio formation energies, expressed in eV, are compared with the Mendelev potential values in brackets. The stars indicate the cases where a different arrangement or final orientation are found with the Mendelev potential.

SIA clusters in Iron

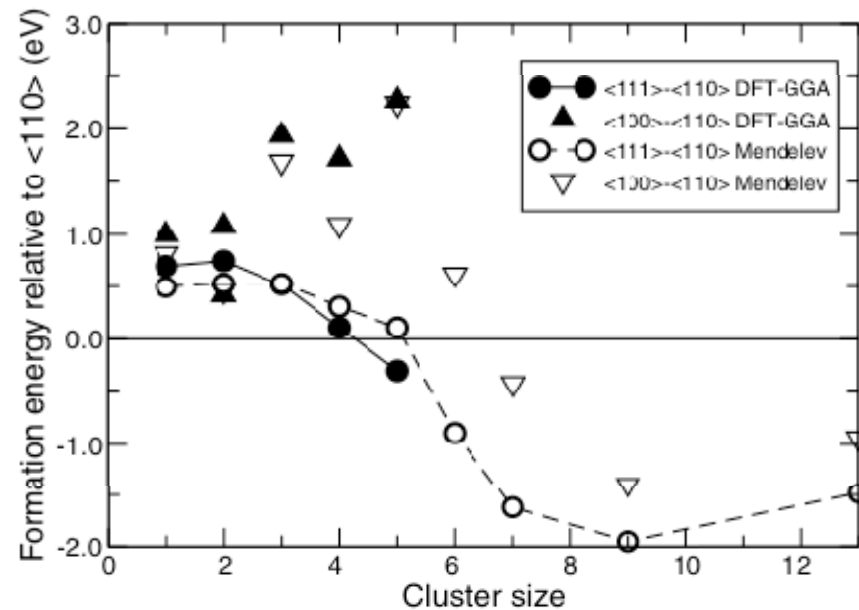


Fig. 5. Size dependence of the stabilities of $\langle 111 \rangle$ and $\langle 100 \rangle$ orientations of the interstitial clusters relative to the $\langle 110 \rangle$ configurations. The differences in formation energies are plotted for the ab initio and the Mendelev potential results. In the $\langle 100 \rangle$ - I_2 case, the two ab initio values correspond to a tilted $\langle 100 \rangle$ and a $\sim \langle 2\ 1\ 1 \rangle$ orientation respectively (see text).

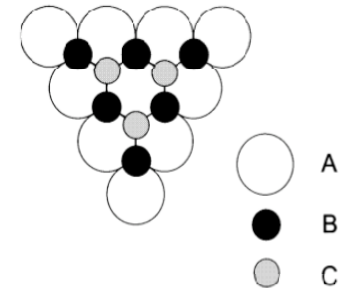
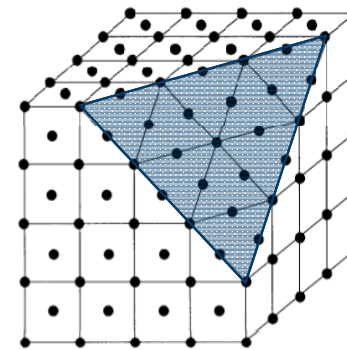
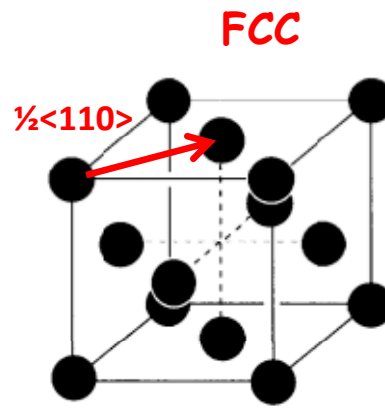
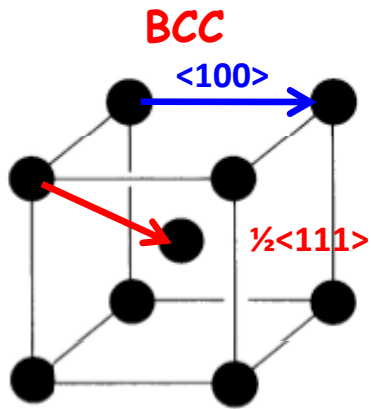
$N_i = 1-4$: $\langle 110 \rangle$ defects

$N_i \geq 5$: $\langle 111 \rangle$ crowdions

- important for dislocation loop type and mobility (see later)

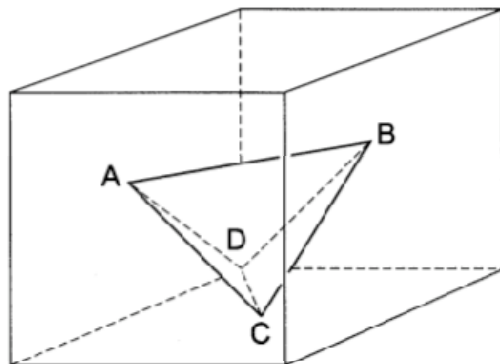
Dislocations and dislocation loops: Burgers vector \underline{b}

As defect clusters increase in size they become dislocation loops (interstitial or vacancy) or SFTs (vacancies in FCC) or cavities (vacancies)



{111} planes: 3-fold stacking sequence
 → faulted loops with $\underline{b} = \frac{1}{3}\langle 111 \rangle$

Stacking fault tetrahedron (SFT)



- Vacancy content equivalent to triangular faulted loop**
- distributed over four {111} triangular faces
 - stacking fault faces + 6 edges of stair-rod partials

for the Department of Energy

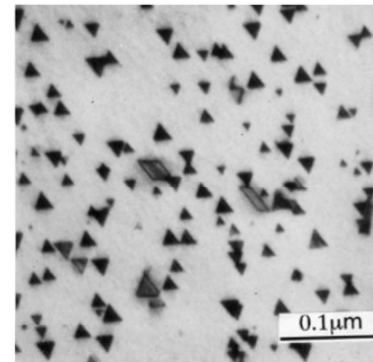
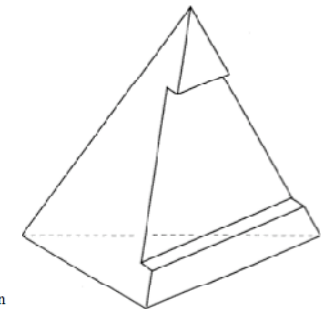
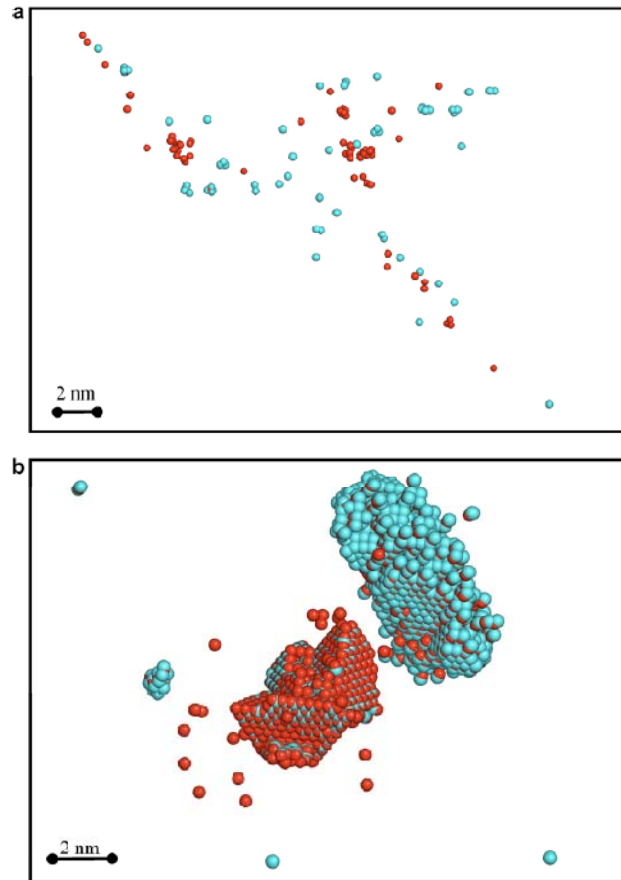


Figure 5.17 Transmission electron micrograph of tetrahedral defects in quenched gold. The shape of the tetrahedra viewed in transmission depends on α with respect to the plane of the foil, (110) foil orientation. *Phil. Mag.* 6, 1351, 1961.)



Growth or shrinkage requires jog lines (ledges)

Examples of defect clusters in Cu formed in MD cascades



Example

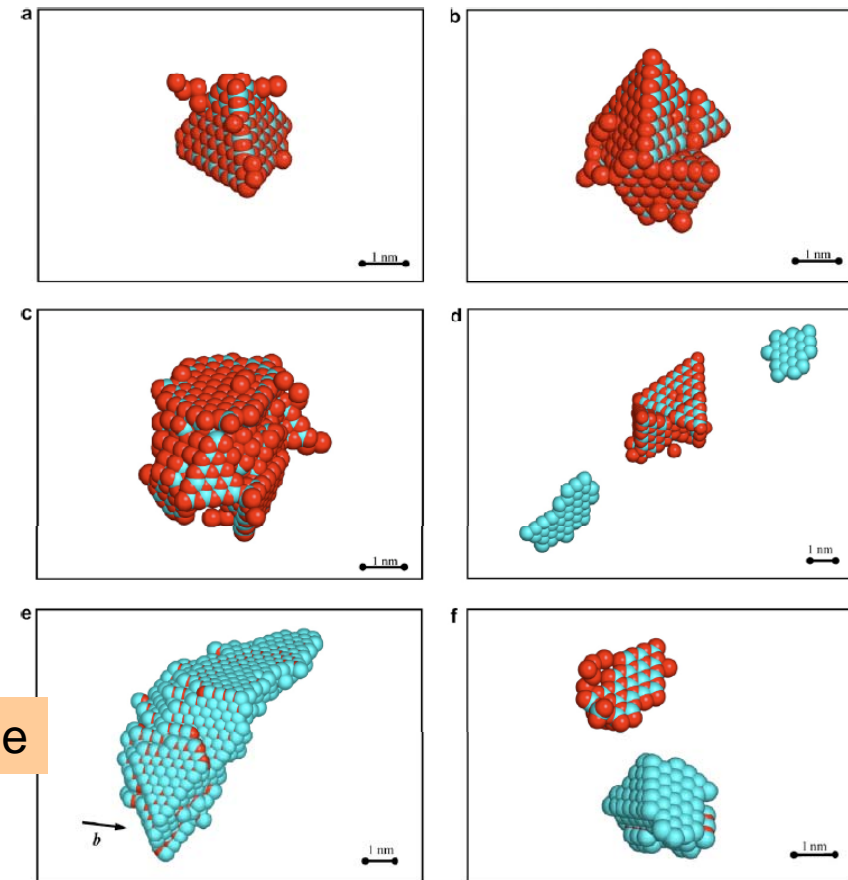


Fig. 6. Typical SIA and vacancy clusters found in displacement cascades. (a) Nearly regular SFT formed by 42 vacancies. (b) Two conjoined SFTs (92 vacancies). (c) Irregular SFT-like vacancy cluster (209 vacancies). (d) Two sessile Frank loops (37 and 22 SIAs) in the vicinity of an SFT-like vacancy cluster (91 vacancies). (e) Glissile SIA dislocation loop of 146 SIAs. (f) Sessile 3-D 45 SIAs' cluster with {111} faces (below) and small SFT-like vacancy cluster of 33 vacancies (above).

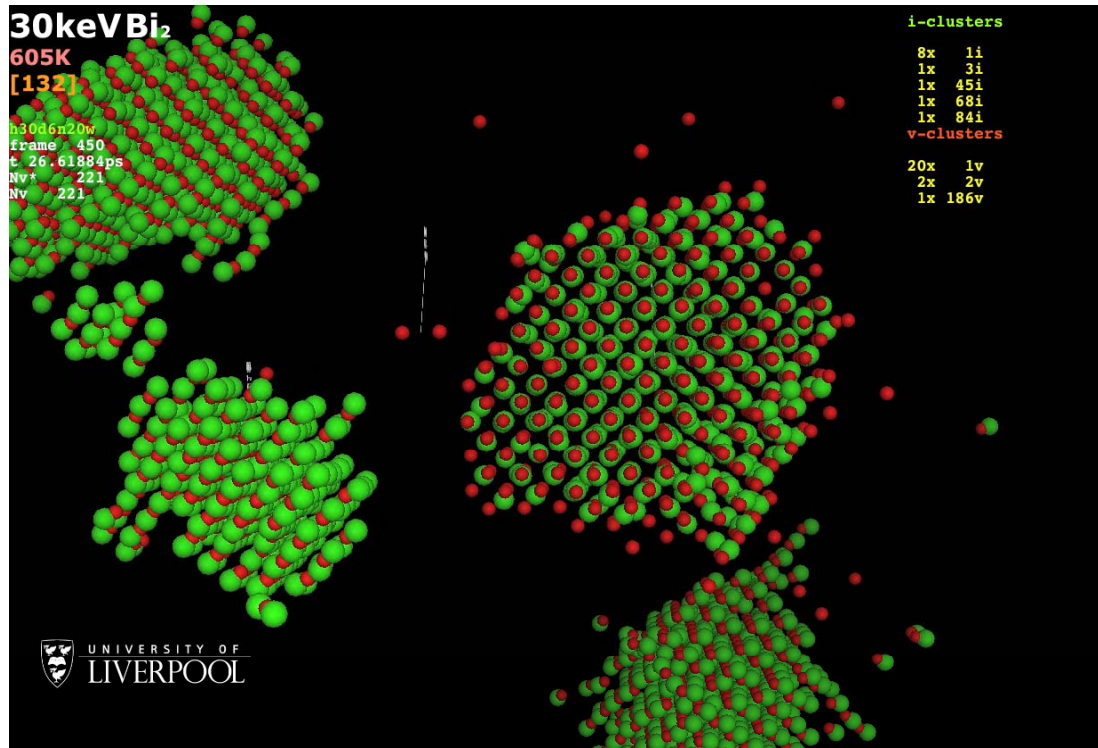
Voskoboinikov, Osetsky & Bacon, J Nucl Mater (2008)

single vacancies and SIAs

+ clusters of SIAs: small dislocation loops $\underline{b} = \frac{1}{3}\langle 111 \rangle$ (sessile) or $\frac{1}{2}\langle 110 \rangle$ (glissile)

+ clusters of vacancies (small cavities or SFT-like arrangements)

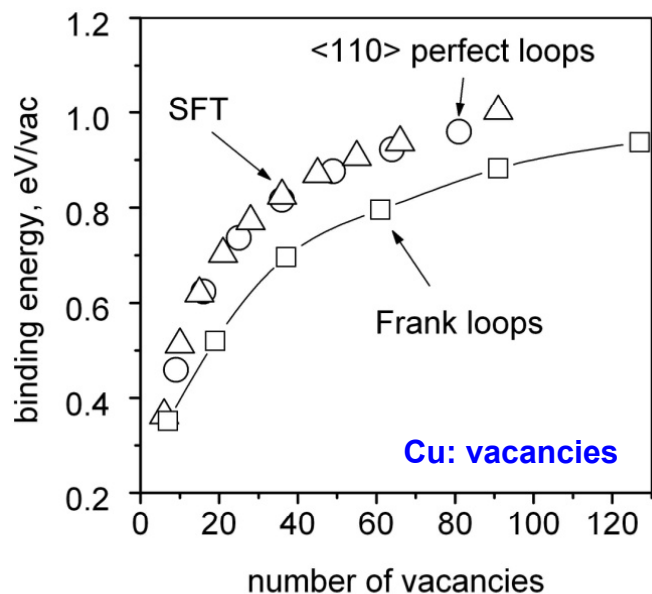
MD simulations of cascade damage in Fe



Calder, Osetsky & Bacon, Phil Mag (2010)

- single vacancies and SIAs
 - + clusters of SIAs: small dislocation loops $\underline{b} = \frac{1}{2}\langle 111 \rangle$ (glissile) or $\langle 100 \rangle$
 - + clusters of vacancies (small cavities or dislocation loop arrangements)

Binding energy of clusters in Cu and Fe



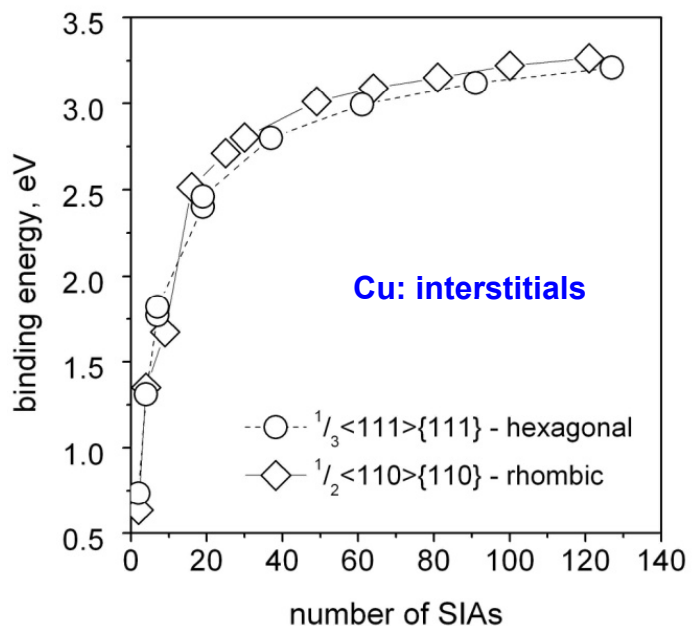
MS simulation

Frank loops have lower binding energy

MD simulation

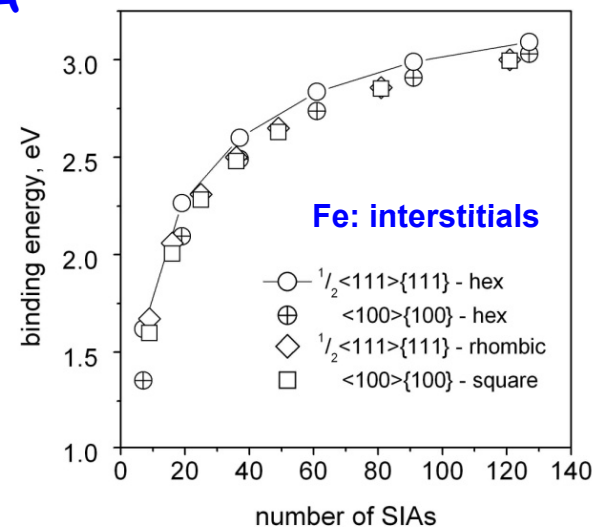
SFT: stable up to 900K for at least 2ns

Frank loops and perfect loops: at $T > 300K$ transform into SFT-like configurations

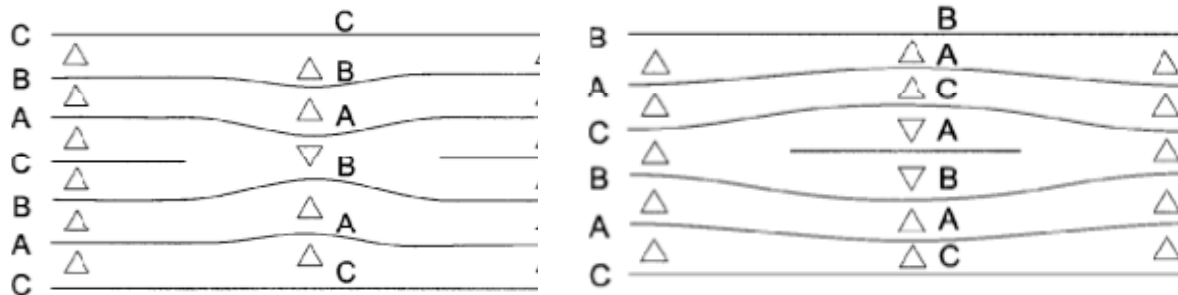


E_b much higher for SIA clusters

Similarly for Fe, but relative stability of $\frac{1}{2}\langle 111 \rangle$ and $\langle 100 \rangle$ depends on interatomic potential



Stability of vacancy and interstitial clusters (dislocation loops)



Loops grow/shrink by climb (absorption or emission of point defects)

Point defect dilatation : $V_r^v \sim -0.2\Omega$, $V_r^i \sim +1.2\Omega$ Formation energy : $E_f^i > E_f^v$

Binding energy of SIAs in interstitial loops $>$ that of vacancies in vacancy loops

(a) Drift mechanism due to dislocation/loop stress field

Superimposed on random migration due to relaxation volume of point defect V_r

For a interstitial loop of radius r_L^i :

$$dr_L^i/dt \propto (+D^i c^i V_r^i - D^v c^v |V_r^v|) ; dr_L^v/dt \propto (-D^i c^i V_r^i + D^v c^v |V_r^v|)$$

Since $D^v \ll D^i$ at temperatures of interest and $|V_r^v| < V_r^i$:

$$dr_L^i/dt \propto +D^i c^i V_r^i \quad \text{and} \quad dr_L^v/dt \propto -D^i c^i V_r^i$$

interstitial loops grow preferentially in point defect flux ('dislocation bias')

Stability of vacancy and interstitial clusters (dislocation loops)

(b) Thermal emission: Interstitial loop can grow by vacancy emission and shrink by interstitial emission. When it does so, its energy increases or decreases by ΔE_L . Thus the formation energy of a point defect at the loop periphery is:

$(E_f^v + \Delta E_L)$ for vacancies; $(E_f^i - \Delta E_L)$ for interstitials

and so the equilibrium concentration of defects at loop periphery is

$$c = \exp[-(E_f^v \pm \Delta E_L)/k_B T] = c_0 \exp[\pm \Delta E_L/k_B T]$$

where c_0 is equilibrium concentration at T

Therefore the rate of change of interstitial loop radius is

$$dr_L^i/dt \propto [-D^i c_0^i \exp(+\Delta E_L/k_B T) + D^v c_0^v \exp(-\Delta E_L/k_B T)]$$

Since $D c_0 \approx \exp[-(E_f + E_m)/k_B T]$, then $D^i c_0^i \ll D^v c_0^v$ and the second term dominates:

$$dr_L^i/dt \propto +D^v c_0^v \exp(-\Delta E_L/k_B T)$$

Similarly $dr_L^v/dt \propto -D^v c_0^v \exp(+\Delta E_L/k_B T)$

Interstitial loops grow preferentially due to vacancy emission at high enough T while vacancy loops shrink

Stability of vacancy and interstitial clusters (dislocation loops)



Finally

$$dr_L^i/dt \propto +D^i c_i V_r^i + D^v c_0^v \exp(-\Delta E_L/k_B T)$$

$$dr_L^v/dt \propto -D^i c_i V_r^i - D^v c_0^v \exp(+\Delta E_L/k_B T)$$

Due to (a) drift interaction & (b) thermal emission:

- interstitial loops are intrinsically stable at all T
- vacancy loops are intrinsically unstable at all T

Some interstitial loops are also glissile (mobile)

- see later

Migration of single point defects and small clusters in Fe

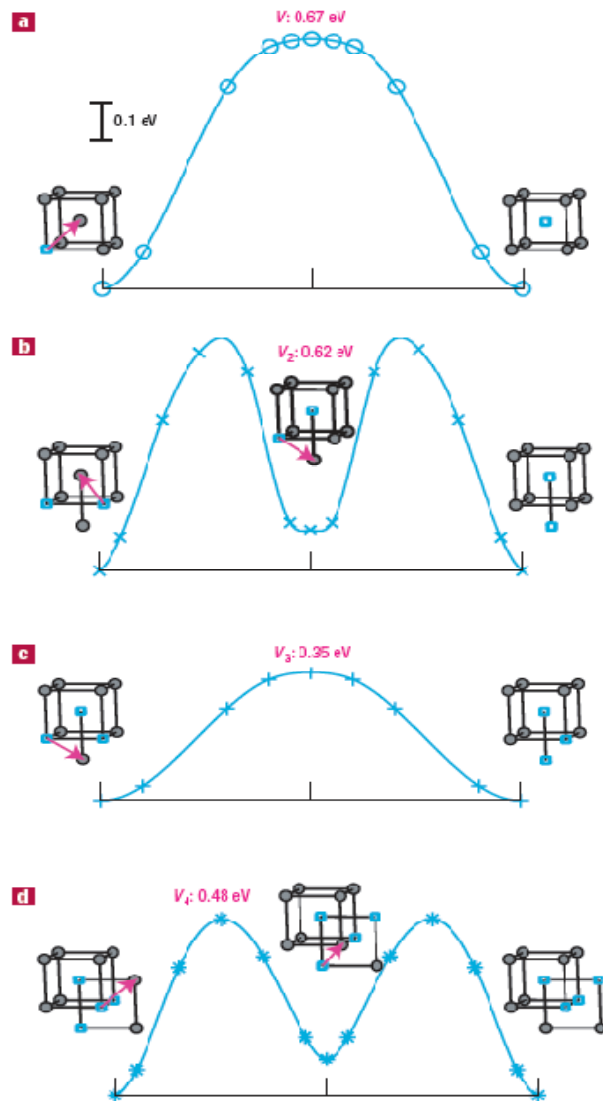


Figure 3 Migration of vacancy-type defects. Energy variation along the most favourable migration pathways for V_1 , V_2 , V_3 and V_4 . The vacant sites are represented by blue cubes, and their migration jumps by magenta arrows. The energy scale is the same as in Fig. 2 for comparison.

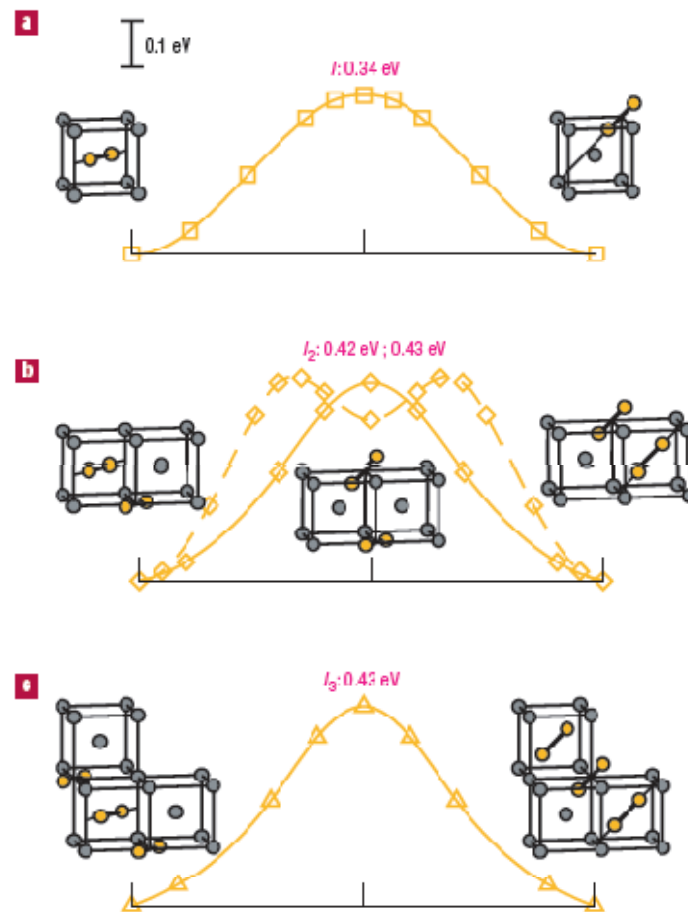
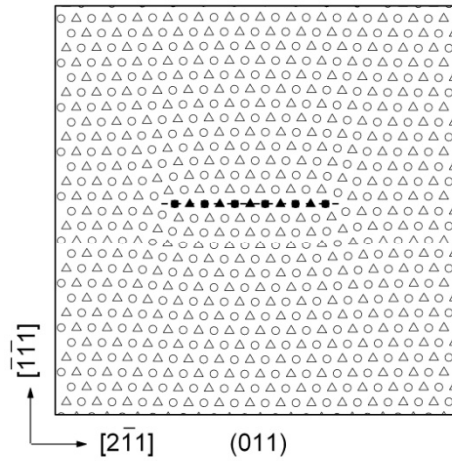
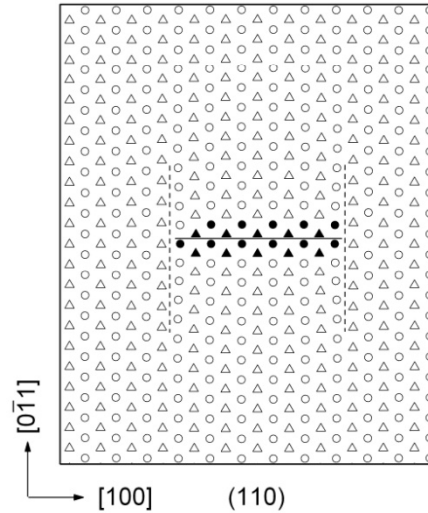


Figure 2 Migration of interstitial-type defects. Energy variation along the most favourable migration pathways for I_1 , I_2 and I_3 , determined by *ab initio* calculations. The corresponding migration energies and schematic representations of the migration mechanisms starting from the defect ground-states are shown: the orange and grey spheres indicate self-interstitial and lattice atoms respectively. The energy scale is the same for all graphs.

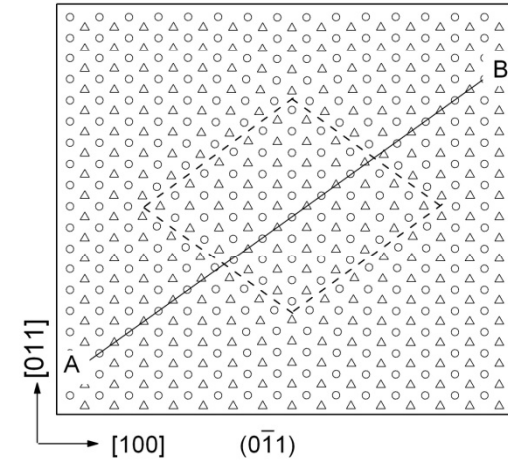
Structure of some SIA clusters in Cu



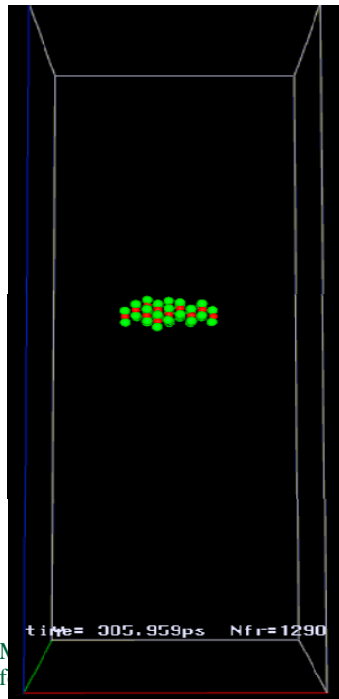
Sessile 37-i Frank loop



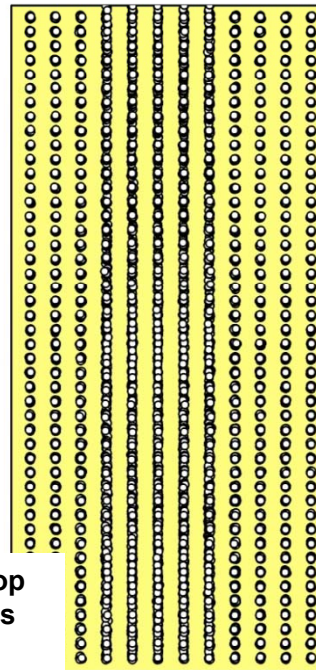
Glissile 36-i $\frac{1}{2}\langle 110 \rangle$ loop



121-i $\frac{1}{2}\langle 110 \rangle$ rhombus loop: **dissociation**

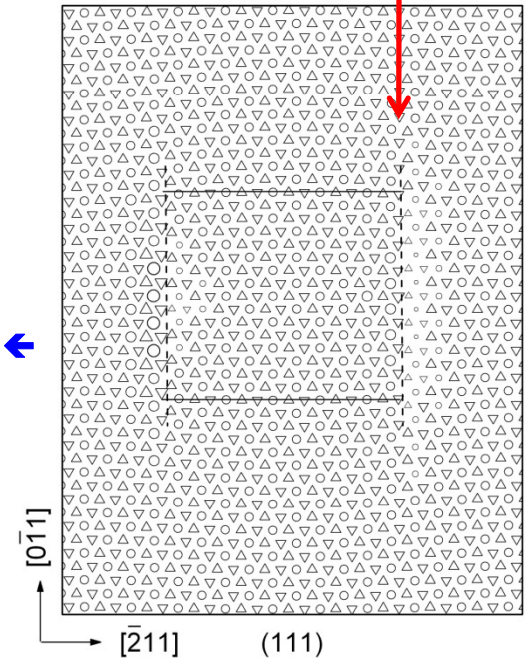


25-i $\frac{1}{2}\langle 110 \rangle$ loop
- atom positions
over 0.8ns at
200K

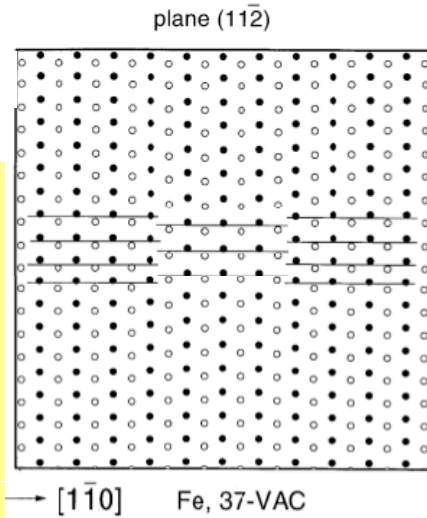
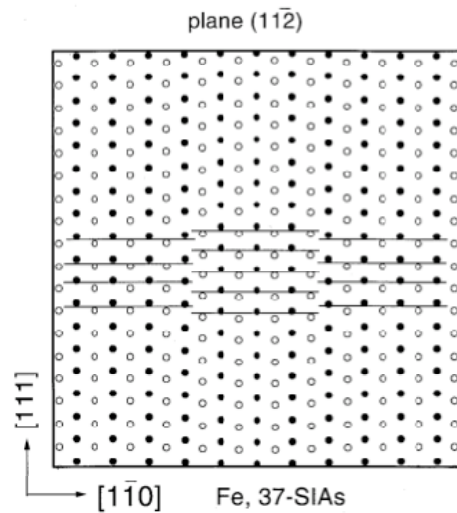


high mobility

low mobility ←

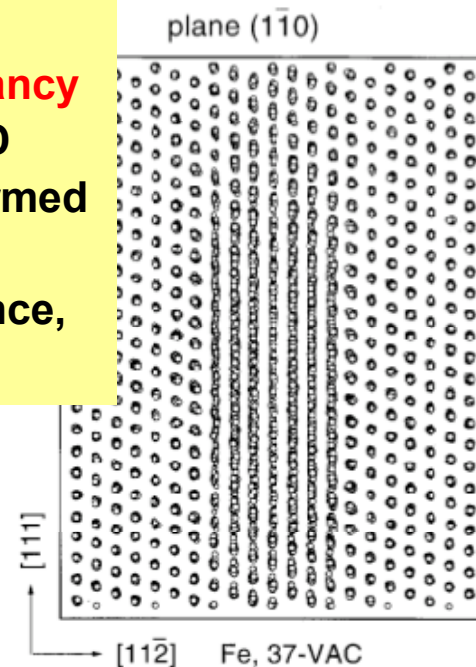
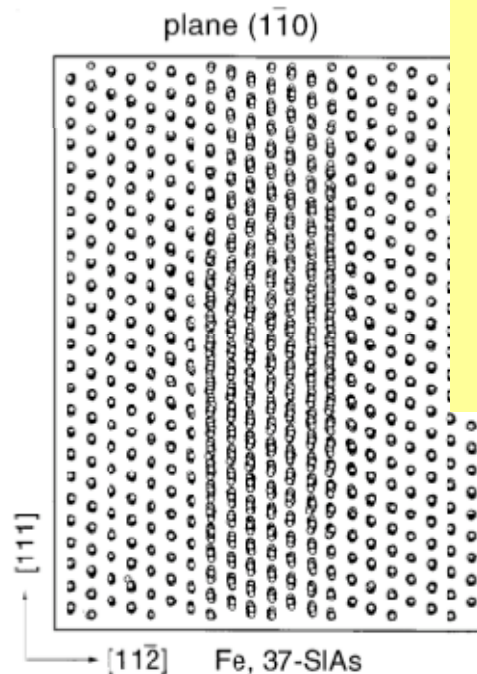


Structure of some clusters with $\underline{b} = \frac{1}{2}\langle 111 \rangle$ in Fe



One dimensional thermally activated glide of **SIA loops** was first observed in MD simulation of cascades (Foreman et al, 1992) and confirmed in experiment treatments (Singh et al 1994) and direct TEM observations (Kiritani, 2000, Arakawa et al, 2005)

One dimensional glide of **vacancy loops** was predicted by MD (Osetsky et al 1999) and confirmed then by TEM experiment (Matsukawa and Zinkle, Science, 2007).



← high mobility →

MD modelling of diffusion due to defects

Iron

Diffusion coefficient: $D = \frac{\langle R^2 \rangle}{2nt}$ ($n = 1$ for 1-D, 3 for 3-D)

- for self diffusion coefficient D^* : $R = R_{\text{atoms}}$

- for defect diffusion coefficient D^d : $R = R_{\text{defect}}$

Tracer correlation factor: $f_{\text{tr}} = \frac{D^*}{D^d}$

= efficiency of defect to produce mass (atomic) transport

Jump frequency analysis (jump length Δ , jump frequency ν):

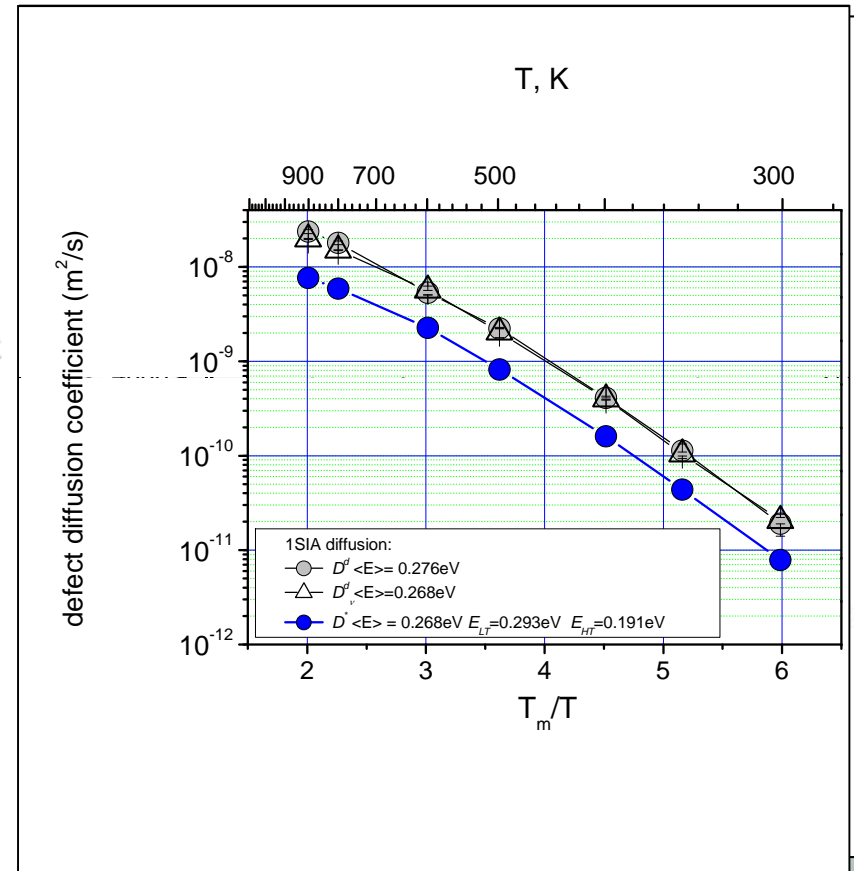
$$D_v^d = f_c \frac{\nu \Delta^2}{2n} \quad \text{- same as } D^d$$

where defect jump correlation factor $f_c = \frac{1 - \langle \cos\theta \rangle}{1 + \langle \cos\theta \rangle}$

and θ is angle between consecutive jumps

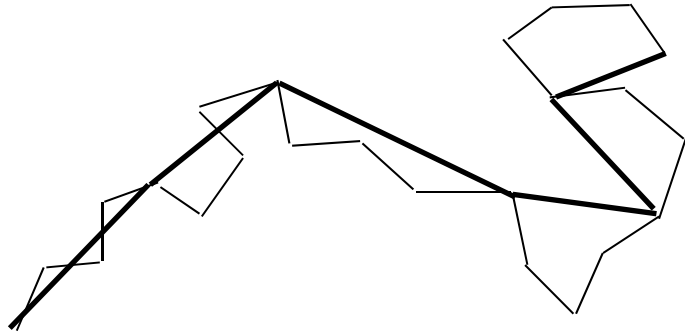
Generally $D = D_0 \exp\left(\frac{-E_a}{kT}\right)$ and $\nu = \nu_0 \exp\left(\frac{-E_a}{kT}\right)$

and E_a different for D^* , D^d and ν due to T-dependence of f



Anento, Serra & Osetsky, Model. Simul. In MSE (2010)

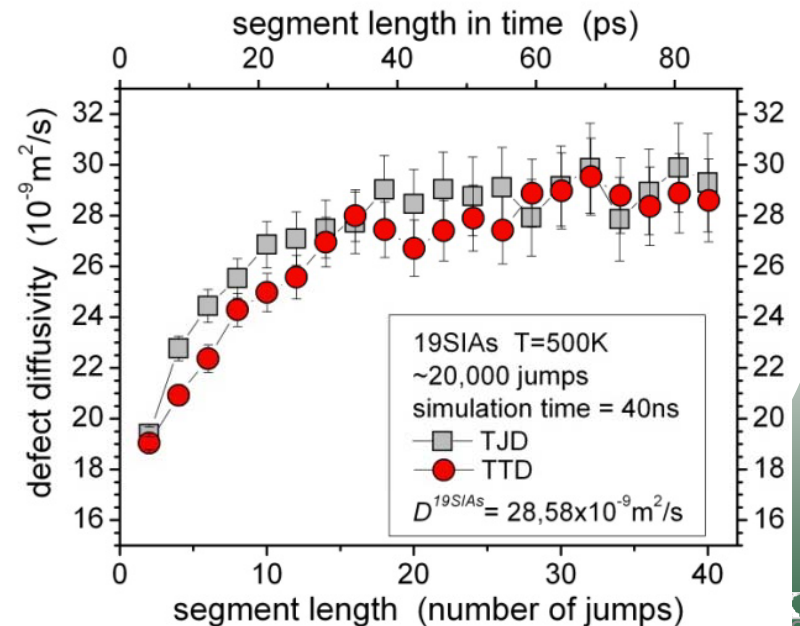
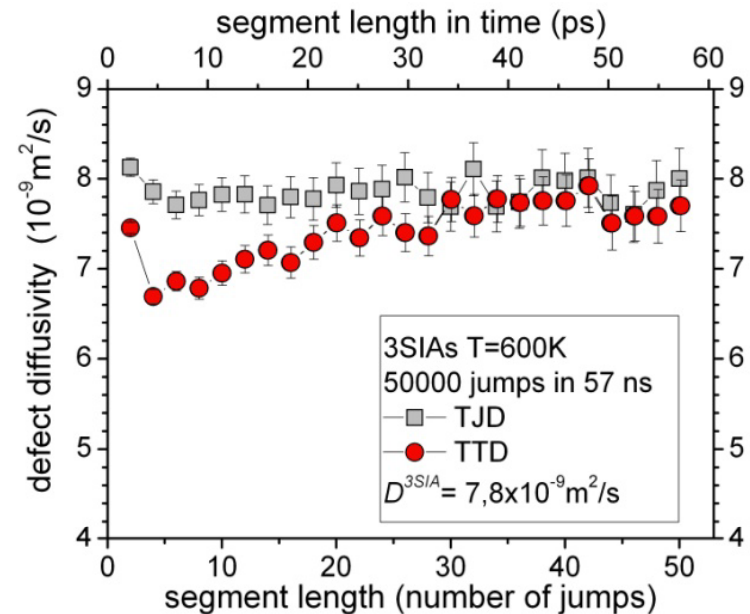
MD modelling of diffusion due to defects



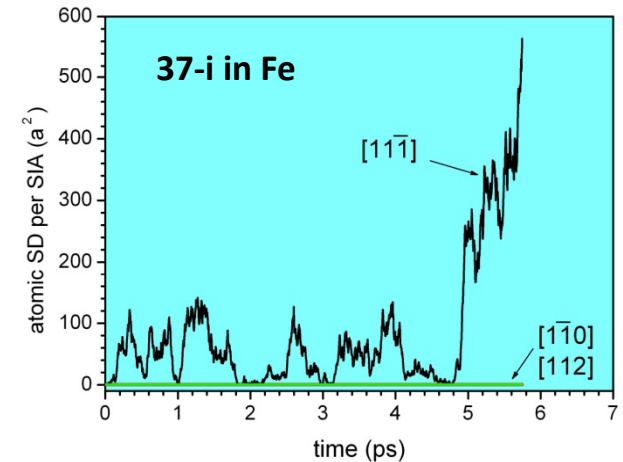
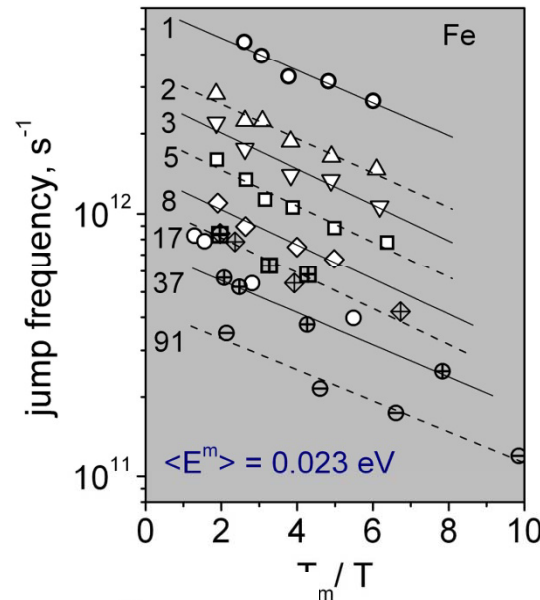
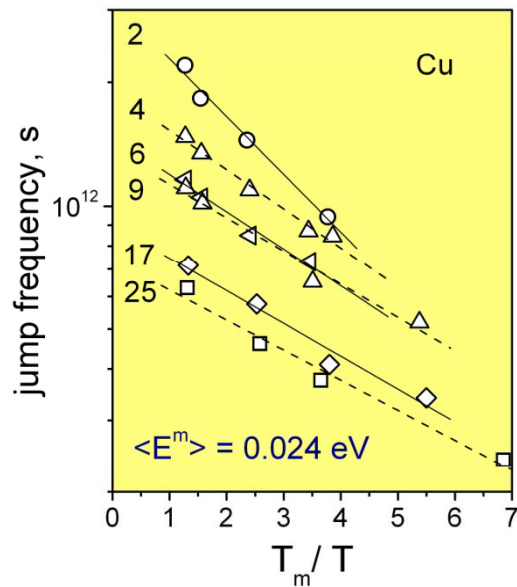
Diffusion coefficient is calculated for each segment and they then are averaged over all segments. If the length of each segment is long enough to include all local correlations and the whole trajectory contain a larger enough number of segments the treatment can be quite successful.

Trajectory decomposition technique
Introduced to improve statistical properties of a single trajectory (Guinan, *Phys. Rev.* 1977)

Later was generalized and improved for 1-D diffusion Osetsky, (2000), Anento, Serra and Osetsky (20010).



Early work (2000) using MD to model migration of SIA defects in Fe and Cu



$$v^n = v_0^n \exp(-E^m/k_B T) \quad v_0^n = v^{crw} n^S, s \sim 0.5$$

- Single and di-SIAs in Cu are dumbbells and move by translation/rotation
- Larger clusters move in 1-D due to stochastic motion of individual SIAs
 - motion is thermally-activated with low activation energy ($\sim 0.02 \text{ eV}$)
- Clustered SIAs in Fe move in 1-D as $\langle 111 \rangle$ crowdions
 - motion is thermally-activated with low activation energy ($\sim 0.02 \text{ eV}$)

Small clusters behaviour depends on the IAP whereas large clusters behave similarly for all the potentials studied.

Some more details on cluster diffusion mechanisms in Fe (Ackland & Mendeleev 2004 IAP):

Migration mechanism:

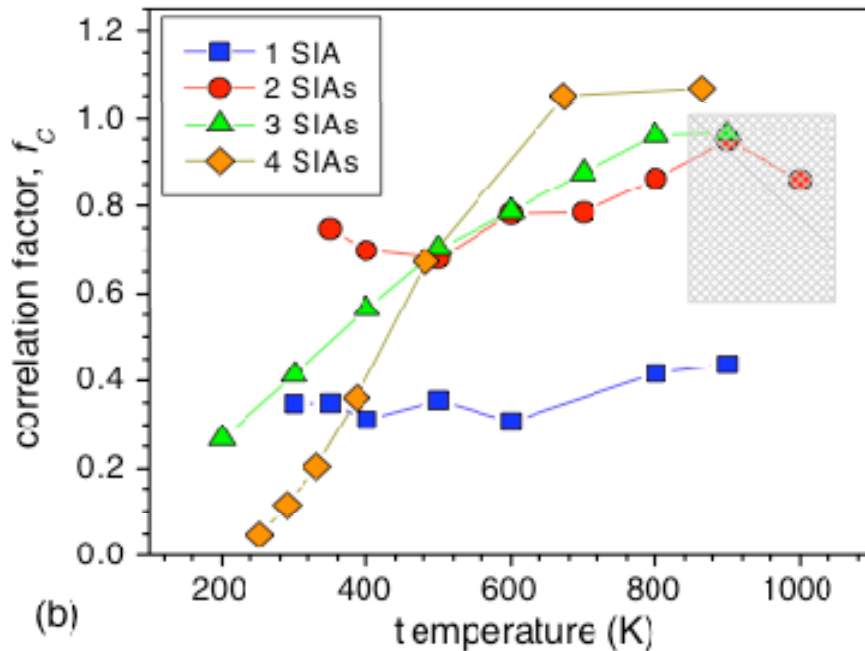
$n = 1-3$: 3-D

$n = 4, 5$: 3-D + 1-D

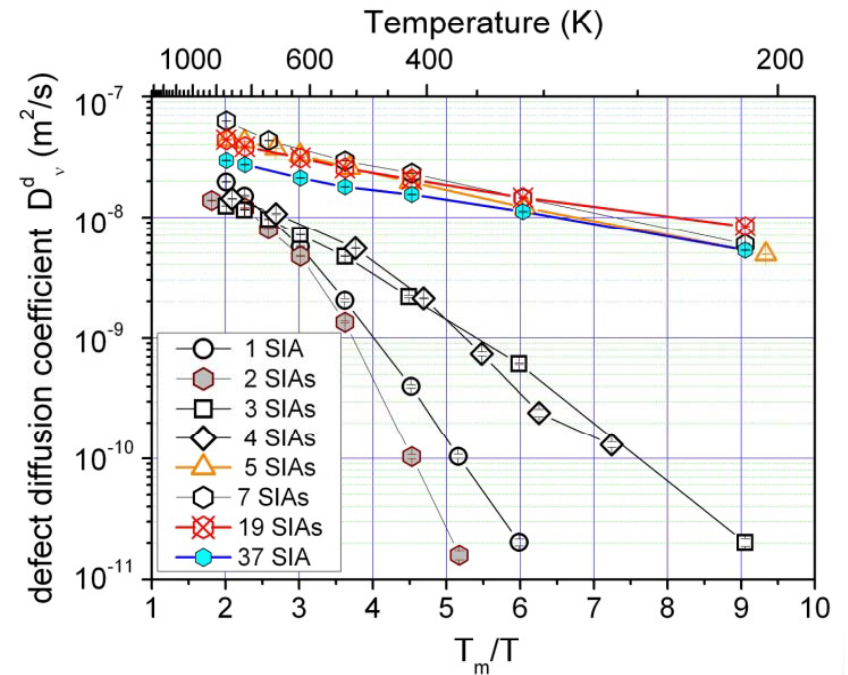
$n \geq 6$: 1-D

For 3-D migration, E_a low at $T > 500$ K

E_a high at $T < 500$ K



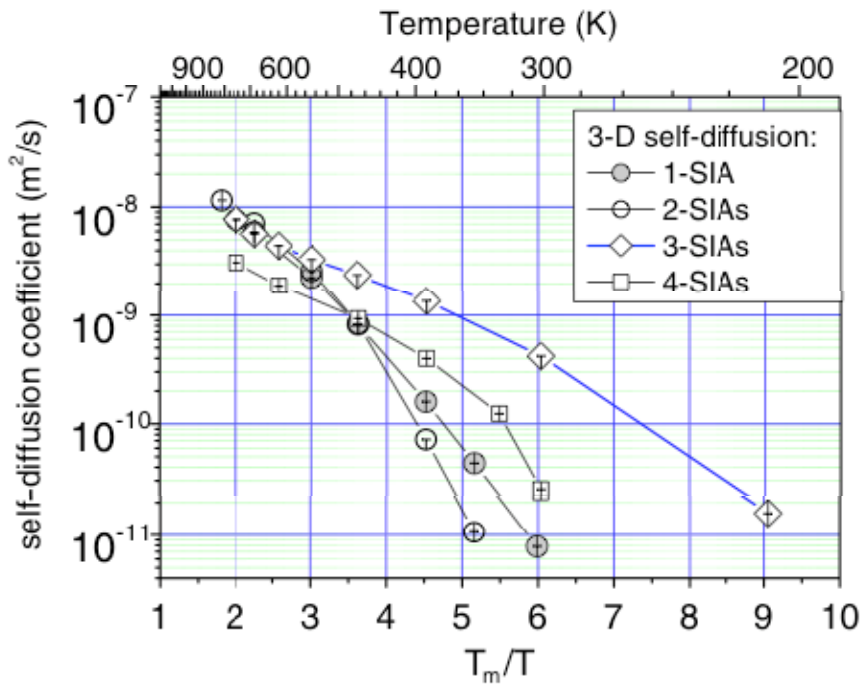
(b)



D^d from jump frequency and f_c

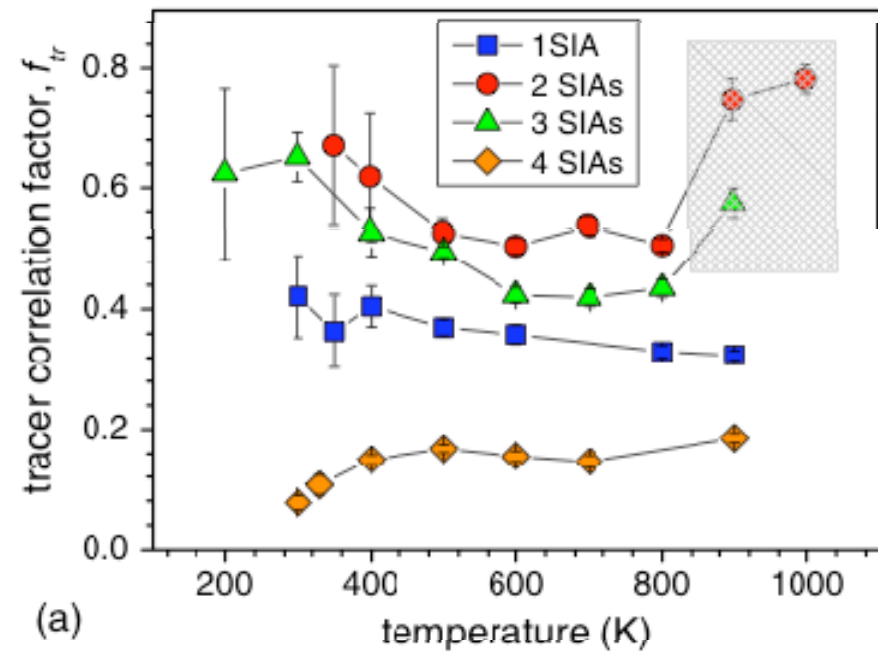
f_c shows change of mechanism with T

MD modelling of diffusion due to defects in Fe



D^* from atom displacements for $N_i = 1-4$

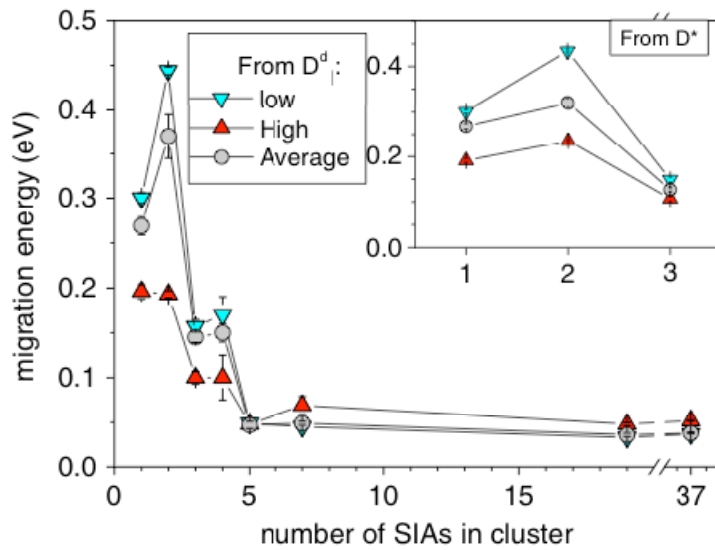
$$D^*/D^d = f_c:$$



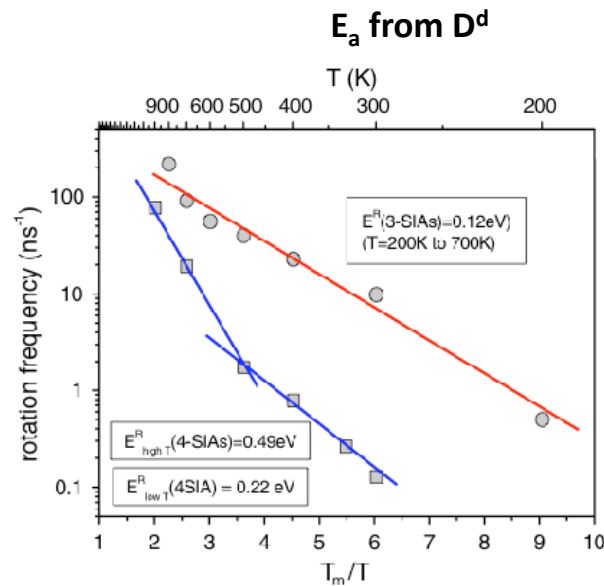
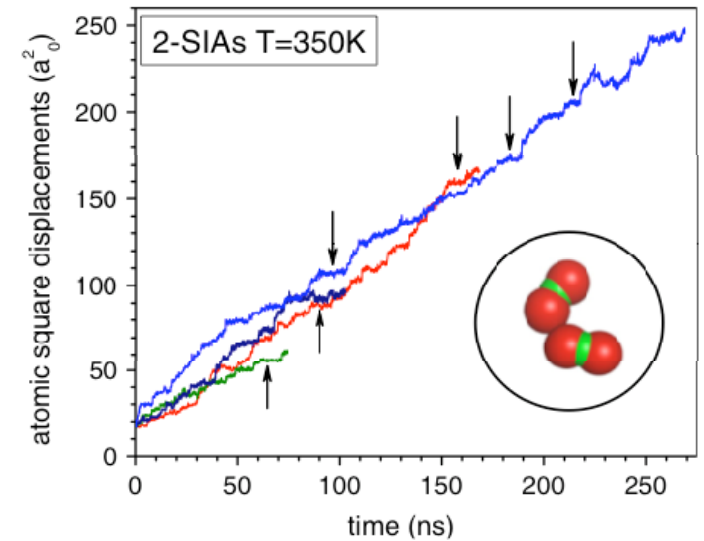
Important conclusion:

mass transport efficiency is decreasing per SIA with increasing N_i !

MD modelling of diffusion due to defects in Fe (cont'd)



- compared *ab initio* values for $N_i = 1-3$ at $T = 0$ K
- increase at low T due to sessile trapping
- E_a saturates at 0.05 eV for $N_i \geq 5$

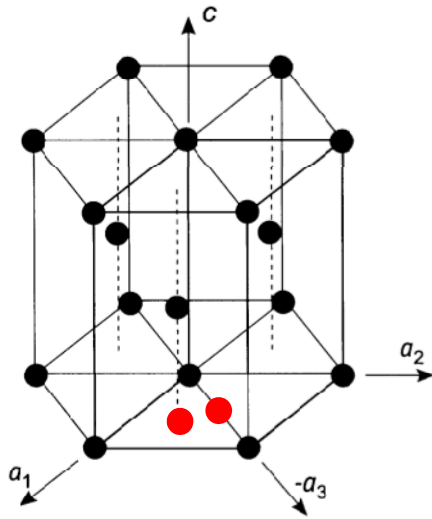


- these move in 1-D segments after rotation to $\langle 111 \rangle$ from more stable $\langle 110 \rangle$

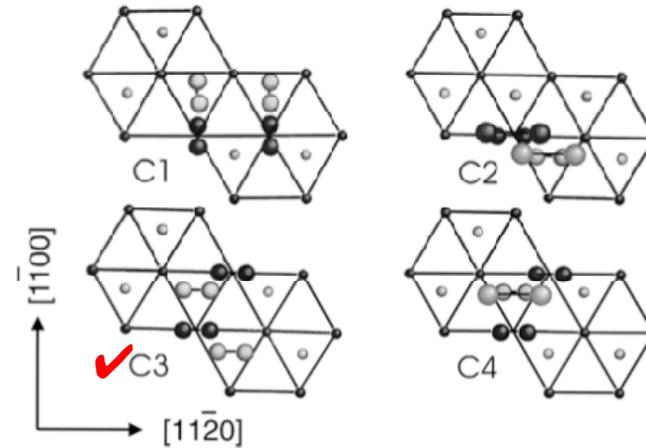
Rotation frequency for 3-i and 4-i

Anento, Serra & Osetsky, Model. Simul. In MSE (2010)

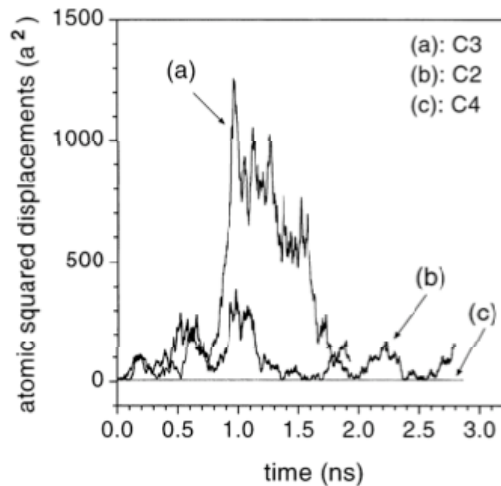
Diffusion anisotropy in HCP, e.g. α -Zr



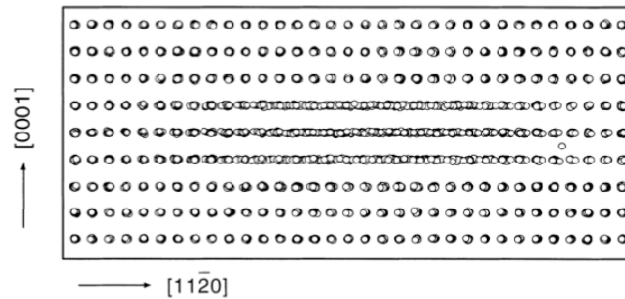
In early models, SIA is BO or BC



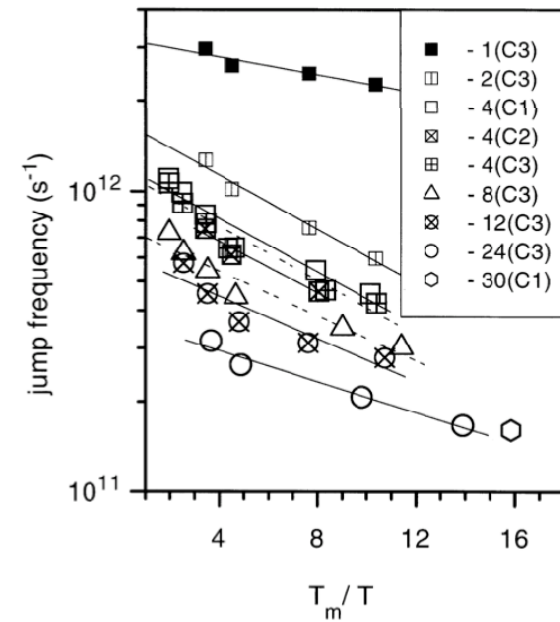
4-SIA clusters: C3 most stable (crowdions)



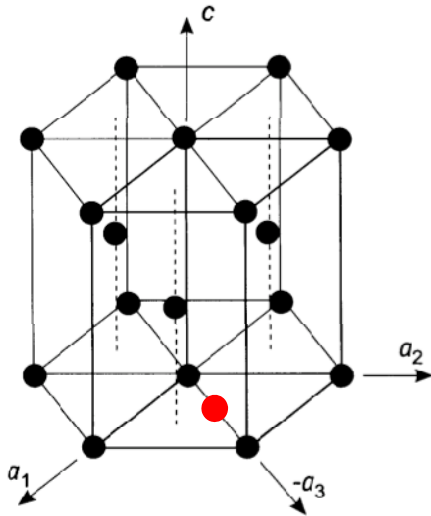
- 4-i clusters at 250 K
- C1 transforms to C3
 - C2 migrates in 2-D
 - C3 migrates in 1-D
 - C4 immobile



24-i cluster (C3) at 250 K
 $E_m = 0.01$ eV for 1-D



Diffusion anisotropy in Zr due to single SIA



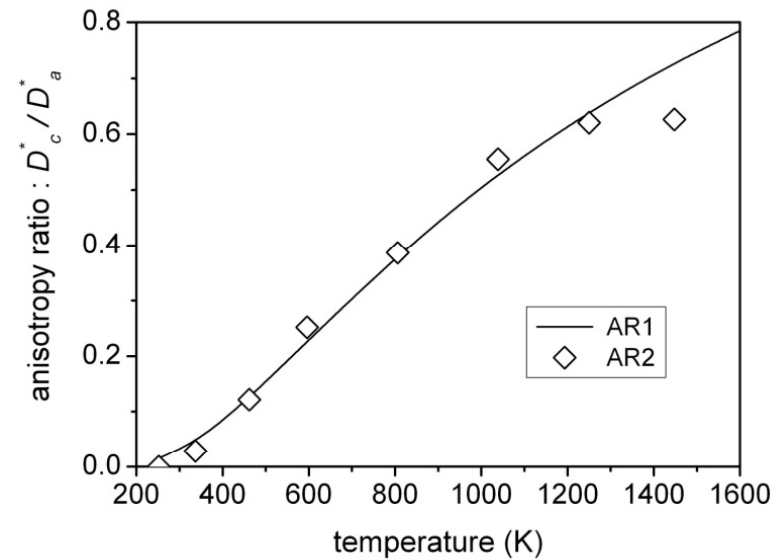
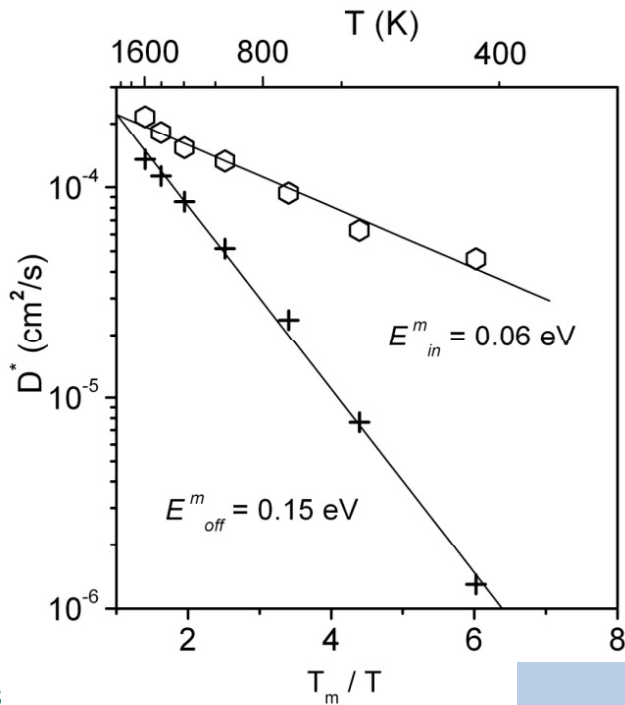
$T < 500 \text{ K}$

- migrates 1-D as basal-plane crowdion with low E_m

$T > 500 \text{ K}$

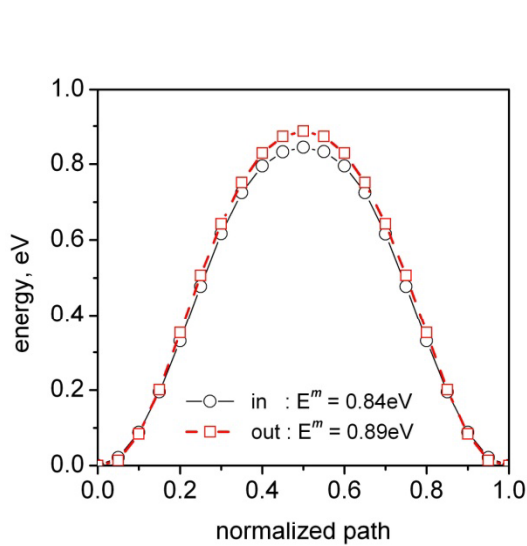
- increasing 2-D (basal) then 3-D migration

This results in strong anisotropy at low T

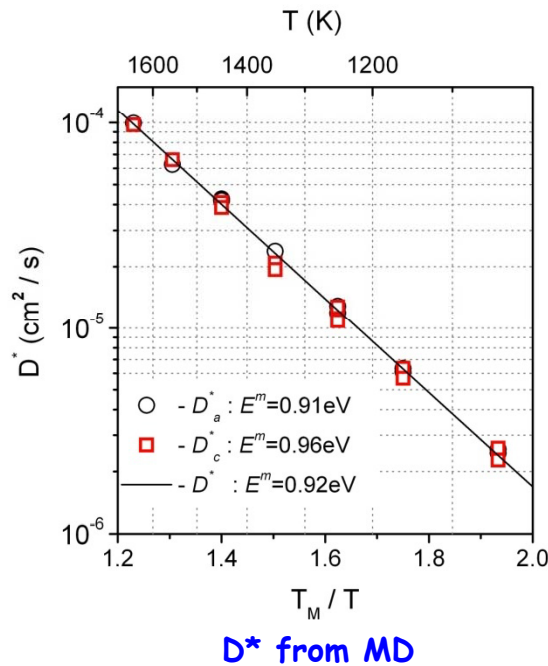


Osetsky, Bacon & de Diego, Metall & Mat Trans (2002)

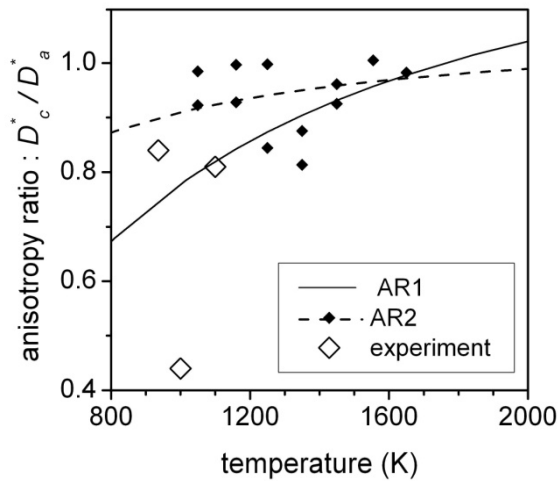
Diffusion anisotropy in Zr due to single vacancy



Migration energy of vacancy at $T = 0\text{ K}$

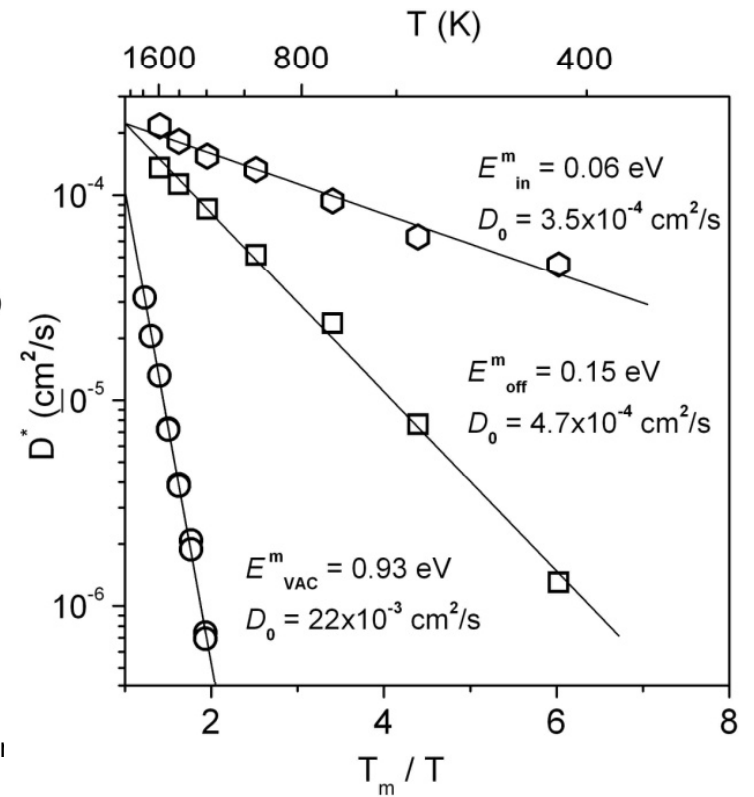


D^* from MD



Anisotropy in self-diffusion due to vacancy mechanism

AR1: from lines for D^* vs $1/T$
 AR2: from MD D^* data for each simulation



Summary of D^* for SIA and vacancy mechanisms

Osetsky, Bacon & de Diego,
 Metall & Mat Trans (2002)

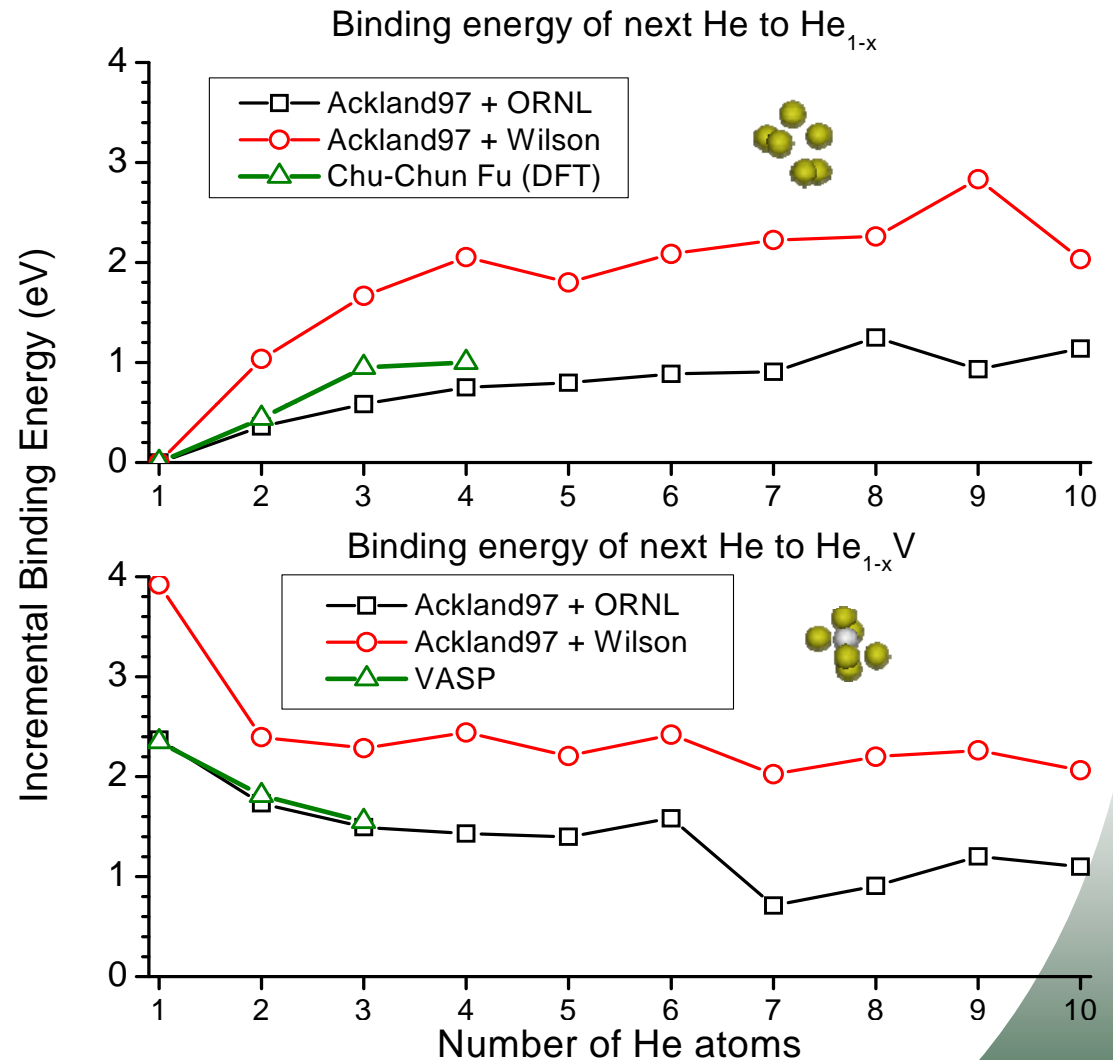


Evolution of He under irradiation:

- properties of He-vacancy defects,
- He transport by single and multiple defects;
- bubble equilibrium;
- He clustering examples

He and He-V Cluster Binding Energy

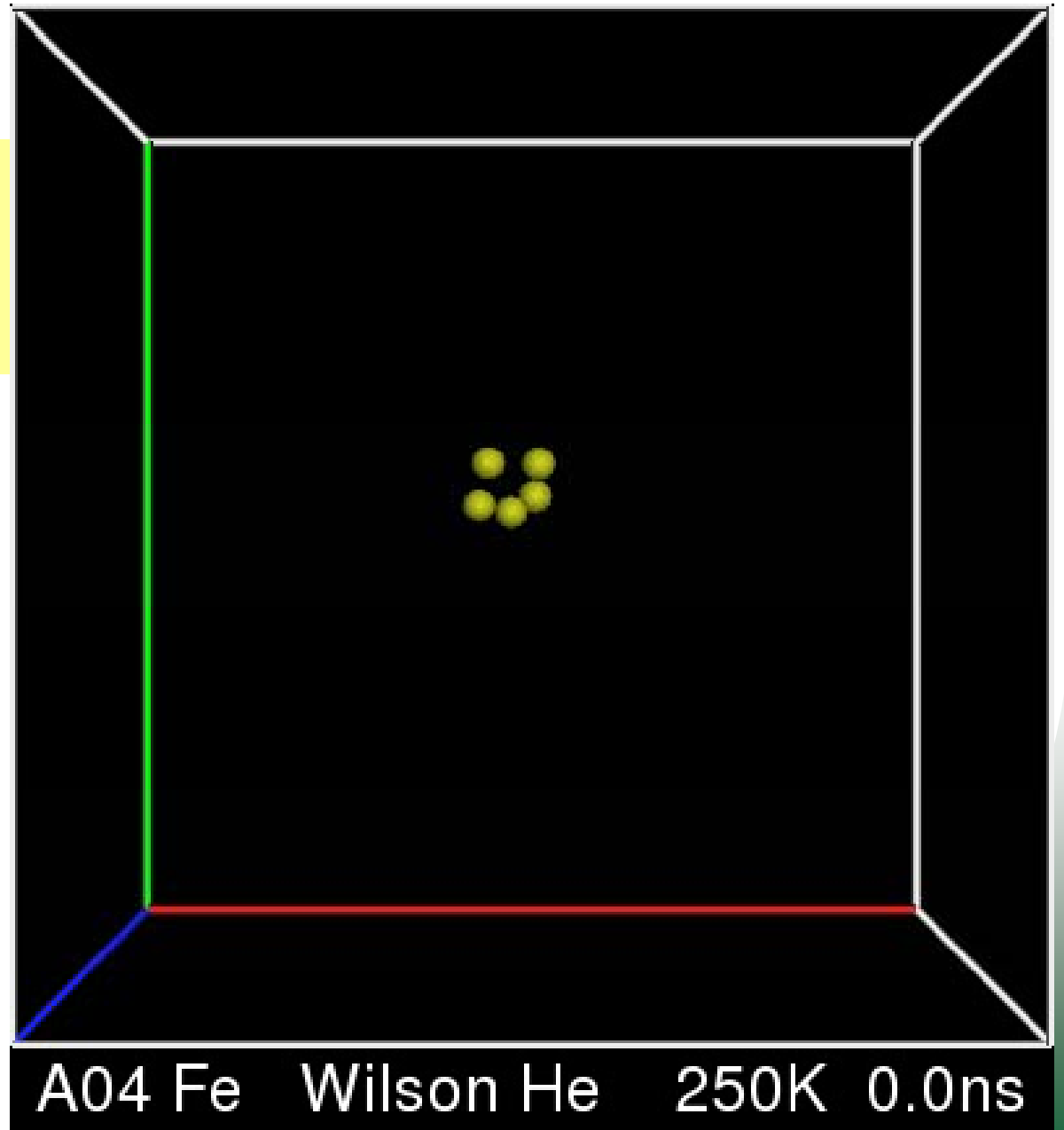
- **Static relaxation**
 - Change in binding energy as another He is added to the defect
- **ORNL 3 body shows:**
 - Better agreement with DFT results
 - Lower B.E. for both He interstitial and He-V clusters
 - B.E. for He interstitial clusters lowered more



Stewart, et al. *Philos. Mag.* (2010)

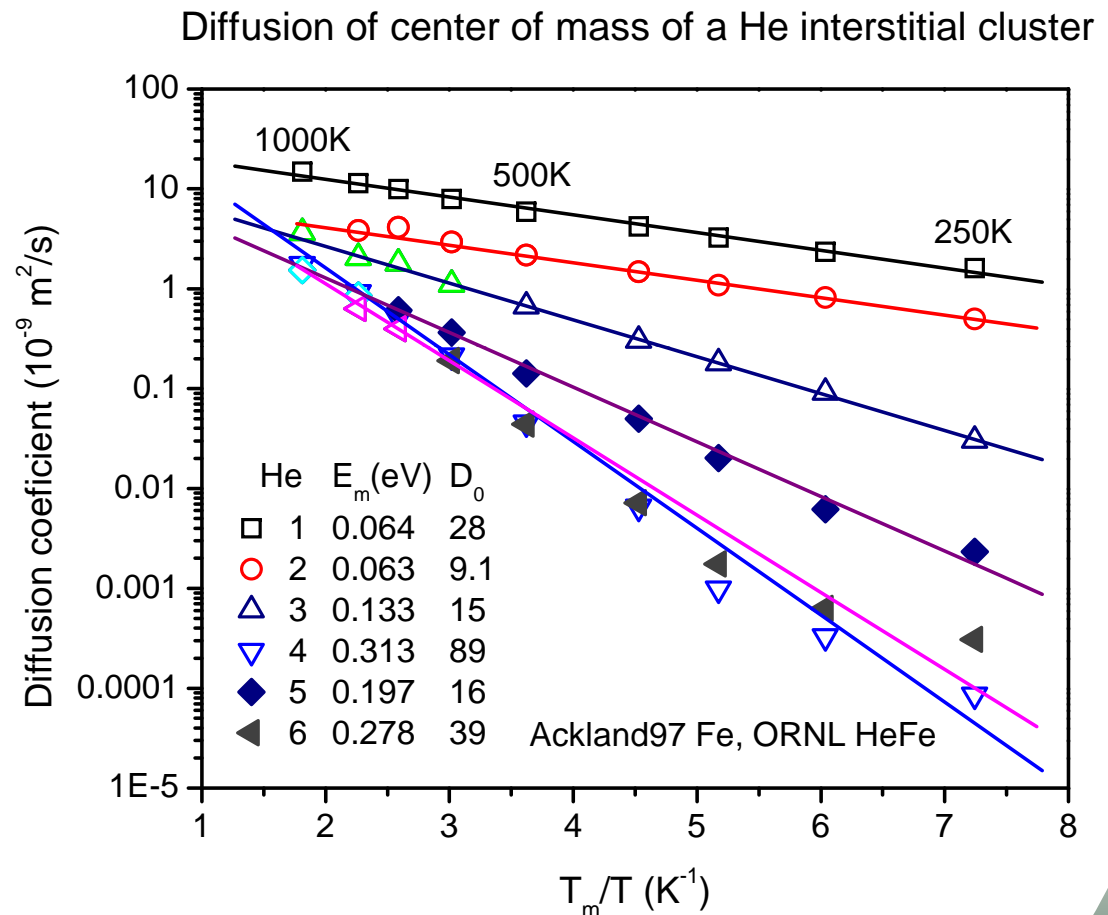
Diffusion of He interstitial clusters

Fast diffusion of He-interstitial clusters is the first example observed so far!



Diffusion of He interstitial clusters

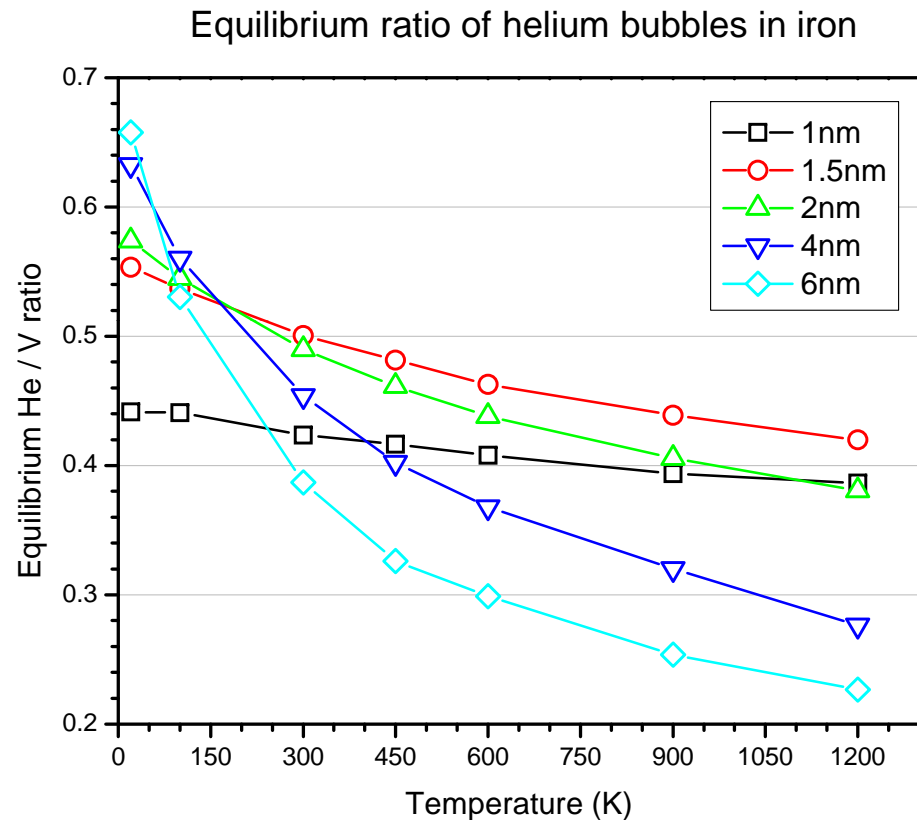
- $\ln(D) = \ln(D_0) - \frac{E_m}{k_B T}$
- **Larger clusters diffuse slower**
 - Except He₄ is slower than He₅ and He₆
- **Open symbols: Cluster remained intact for the entire 15-30ns simulation**
- **Solid Symbols: Cluster dissociated or ejected an SIA**



Stewart, et al. *J. Nucl. Mater.* (2010)
ICFRM-14 Conference proceedings

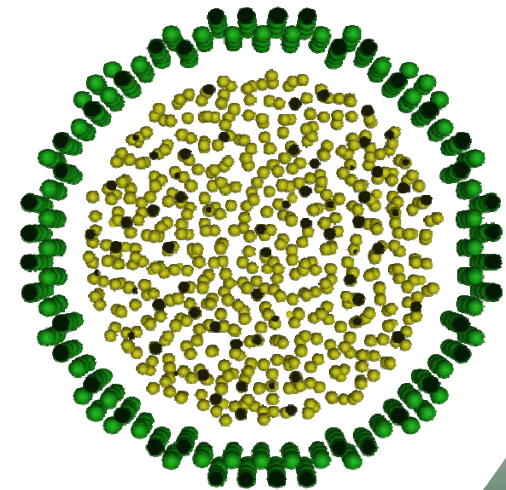
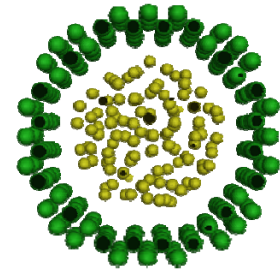
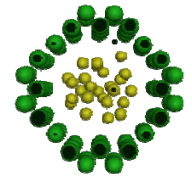
Equilibrium He/V ratio in bubbles

- The He/V ratio at which the dilation curve crosses zero is plotted
- As bubble gets smaller, gap becomes more important
 - At 1.5nm, gap is ~50% of the volume



Helium bubbles

- Simulated 1, 1.5, 2, 4, 6nm bubbles
 - Gap observed
 - Fe surface dilates in/out dep. on He/V ratio
 - Equilibrium \equiv zero dilation
- Eqb. ratio depends on T and d
 - Maximum near 1.5nm due to gap
 - At low T, larger for larger bubbles

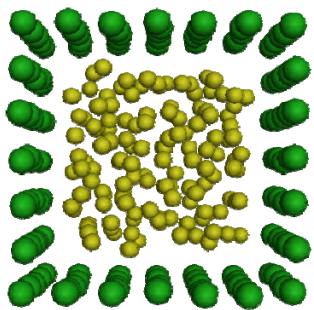


Stewart, et al. *J. Nucl. Mater.* (2010)

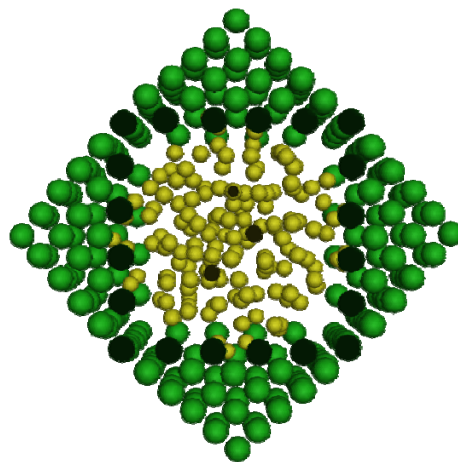
ICFRM-14 Conference proceedings

Effect of facets

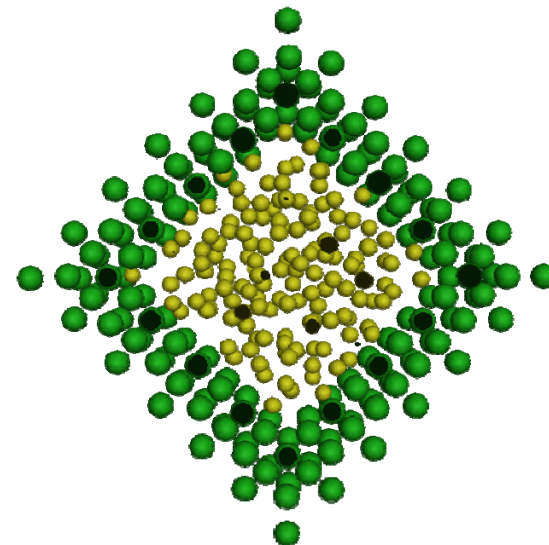
- Create a polyhedral 'bubble' that consists of only one type of surface.
 - Investigate the effect of surface type on equilibrium



{100} faces



{110} faces

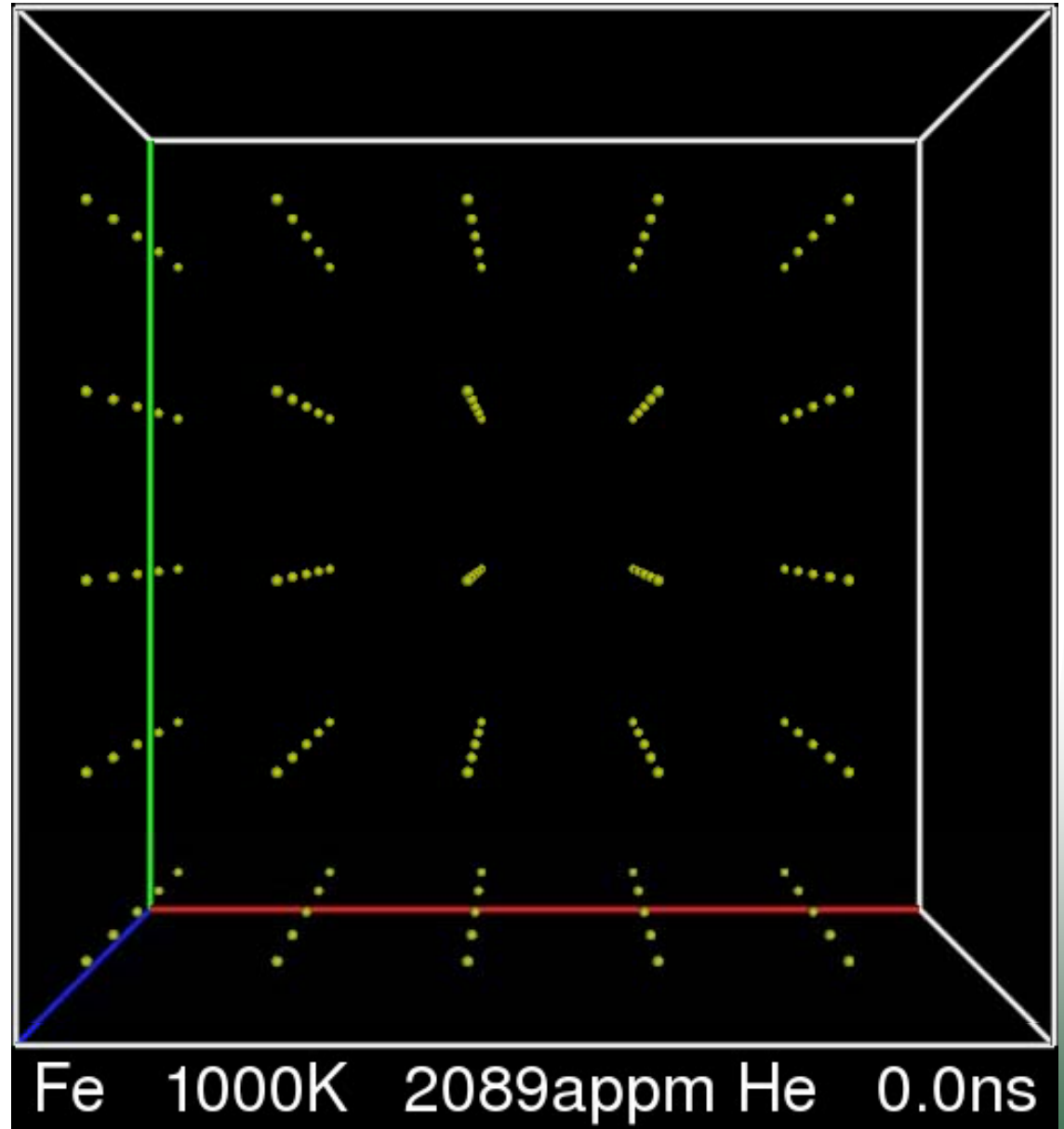


{111} faces

He coalescence: MD simulations

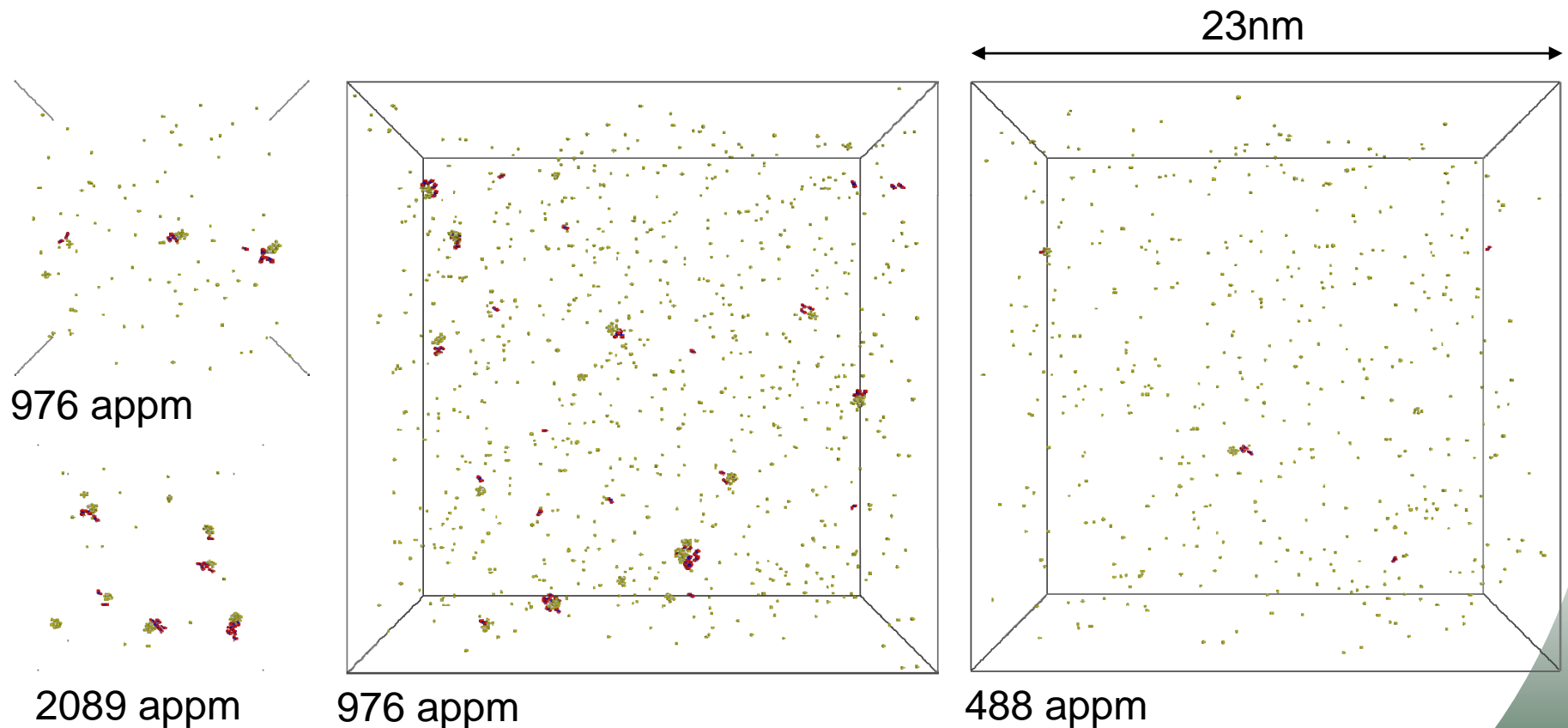
- 125 He atoms in box of 60,000 Fe atoms at 1000K
- He atoms coalesce into clusters
- Clusters push out SIAs
- Some SIAs trapped near He-V clusters
- Multiple trapped SIAs line up and form dislocation loops

Stewart, et al. *Philos. Mag.* (2010)



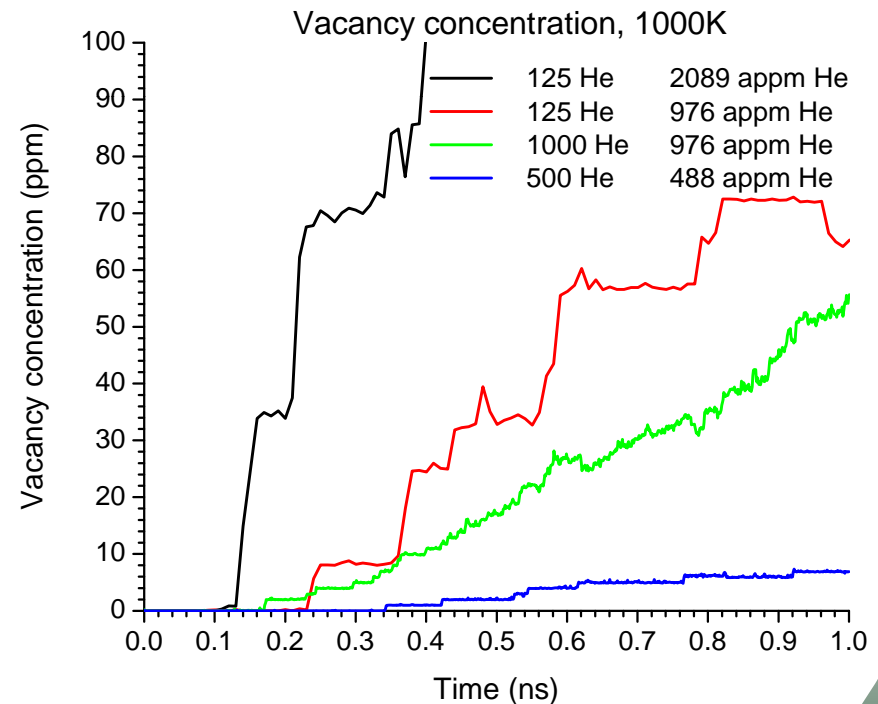
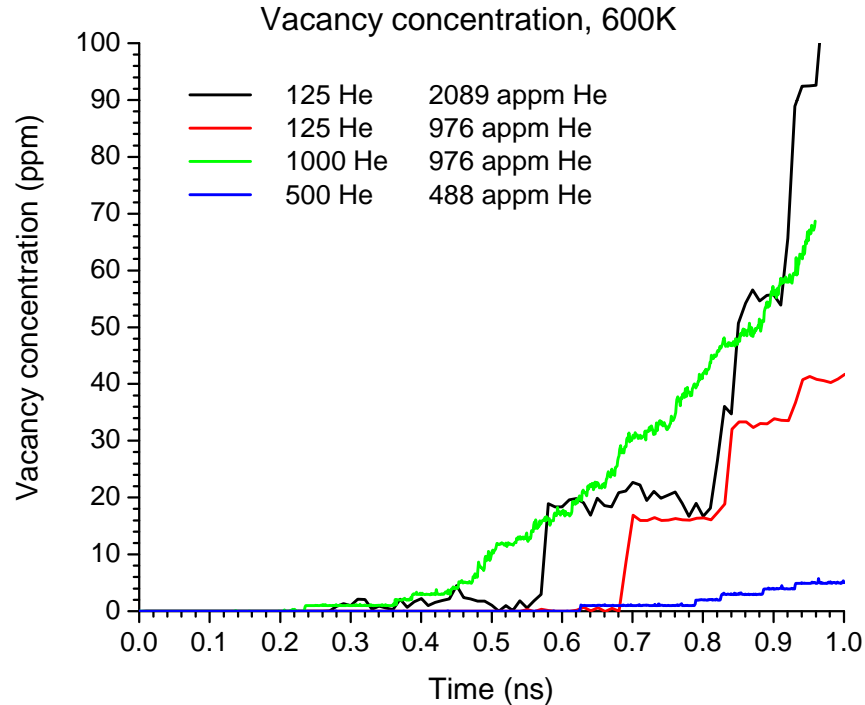
He coalescence: MD simulation

1,024,000 Fe atoms, $T = 1000\text{K}$, Time = 1ns



He coalescence: MD simulation

- Lower concentration gives fewer but bigger clusters



Other mechanisms (known but not covered here):

1. Interactions involved SFTs in fcc metals:

SFT is a vacancy type defect and a very unique object - it is rather stable, does not shrink in interactions with SIAs or clusters (no recombination) and does not grow in interactions with vacancies!!!

2. Interactions between glissile SIA loops and edge dislocations:

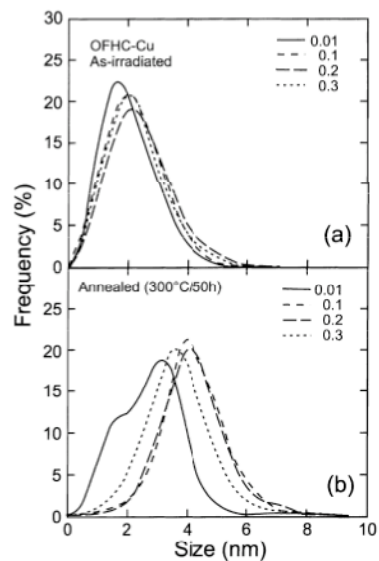
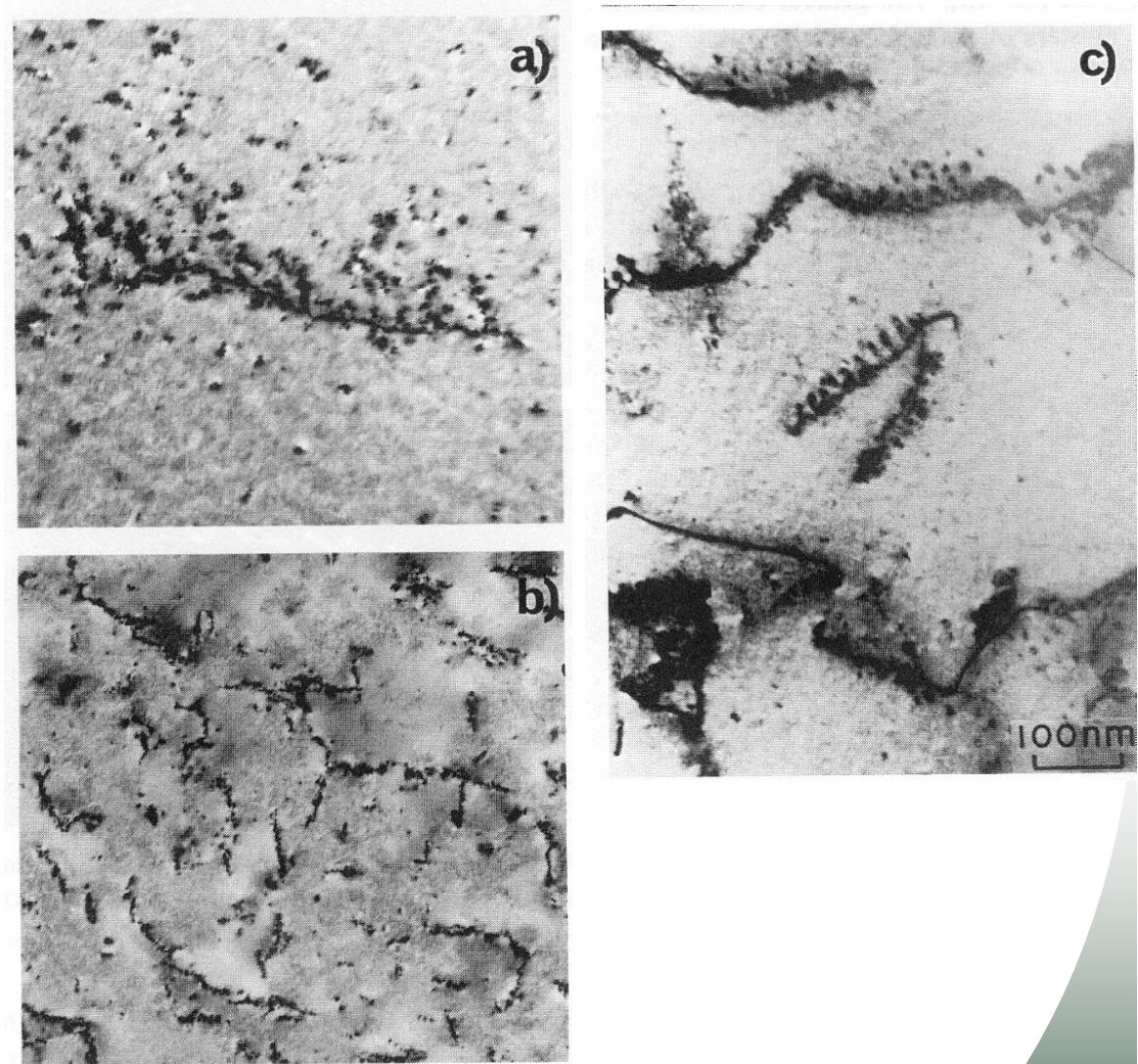
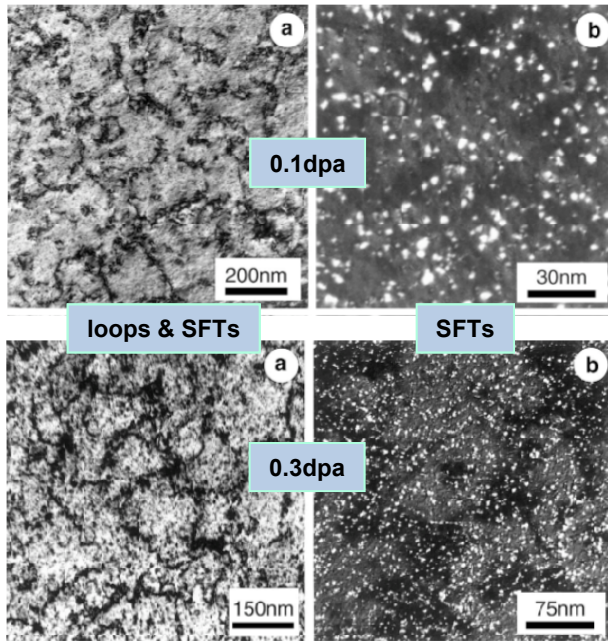
- dislocation decoration or loop segregation on dislocations introduces a significant inhomogeneity in the microstructure

3. Interactions between glissile SIA loops:

- loop coalescence
- change of the loop Burgers vector
- rafts creation

Motivation: effect of irradiation microstructure on mechanical properties

Cu, n-irradiated at 100°C (Singh et al. JNM 2001)



ORNL Department of Energy

Decoration & rafts: Mo [n]
 - Singh & Evans (1997)
 - Yamakawa & Shimomura (1998)

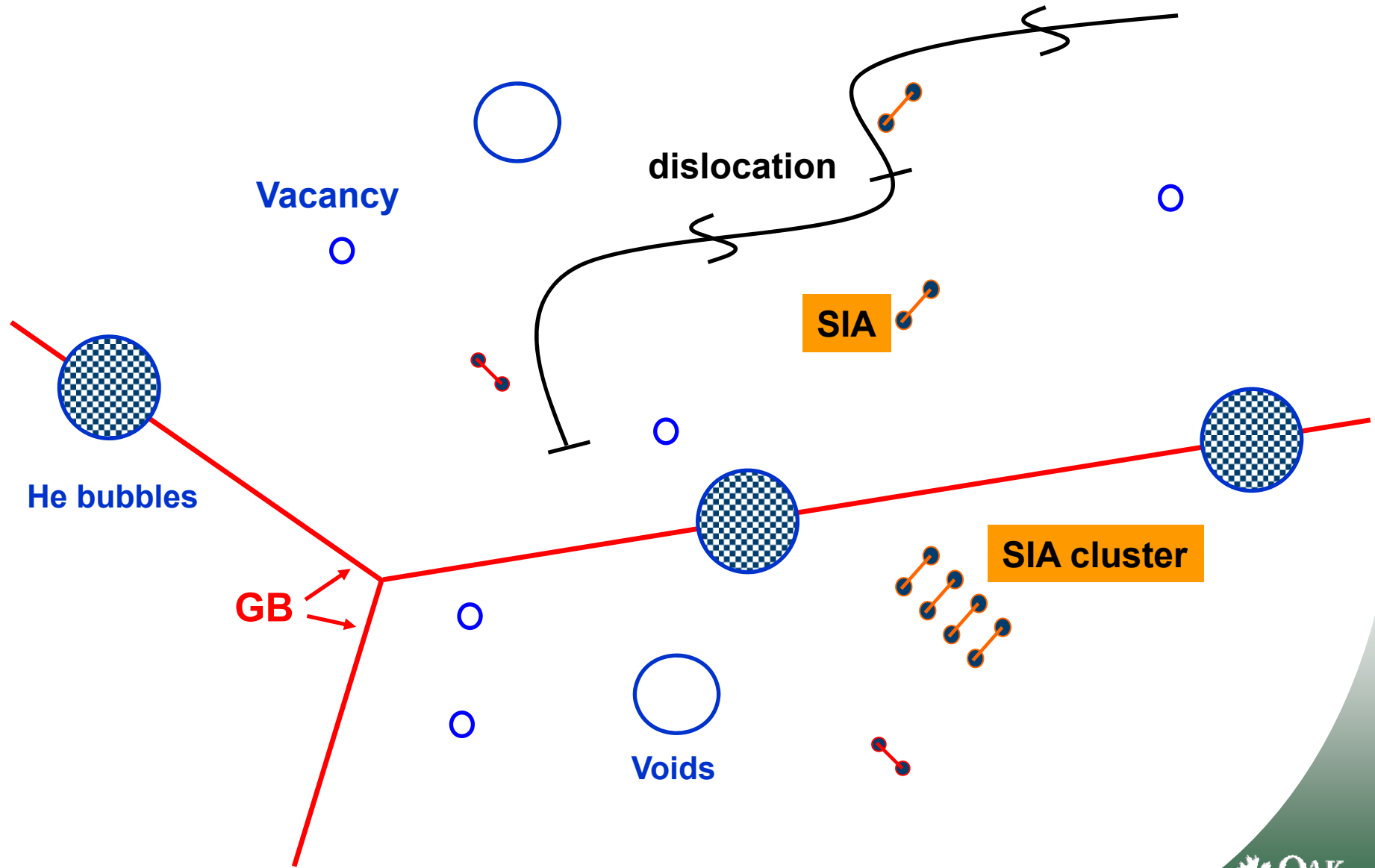
There are number of other mechanisms that are important in many particular cases of microstructure evolution ==>>

There is a significant need in understanding atomic-scale details of defects properties and reactions!

Radiation effects as microstructure evolution:

- Irradiation induces new defects at a level significantly above thermodynamically defined level
- Some defects i.e. SIA clusters, He-clusters, etc. appear only at irradiation conditions
- Evolution of radiation induced defects and their interactions between themselves and existing microstructure lead to significant change in the total material's structure that defines change in physical properties
- Defects mobility is the main mechanism of radiation induced microstructure evolution

Radiation effects as microstructure evolution:



Microstructure evolution: general approach

The most general form of diffusion equations for mobile defects:

$$\frac{dC_v(r,t)}{dt} = D_v \Delta C_v(r,t) + (G_v(r,t) + G_v^T) - \mu_R D_i C_i(r,t) C_v(r,t),$$
$$\frac{dC_i(r,t)}{dt} = D_i \Delta C_i(r,t) + G_i(r,t) - \mu_R D_i C_i(r,t) C_v(r,t).$$

Boundary conditions:
 $C_v(S_j) = C_v^{eq}, j = 1 \dots n$
 $C_i(S_j) = C_i^{eq},$

Here: $C_v(R, t)$ and $C_i(R, t)$ vacancy and interstitial concentration at vector R and time t ; D_v and D_i - diffusion coefficients, $G_v(R, t)$ and $G_i(R, t)$ - generation of vacancies and interstitials and μ_R is a mutual recombination coefficient.

These include only evolution of existing defects but not nucleation. Defect (void, dislocation loops, secondary phase precipitates) nucleation is a kinetic process not considered here.

Generally the above equations have to be solved in a crystal with different type of defects: voids, dislocations and dislocation loops, secondary phase precipitations, etc. located at positions determined by the radius vectors $\{R_1, R_2 \dots R_n\}$ where n is a total number of absorbing defects.

Radiation Damage Accumulation and Radiation Damage Theory

Radiation damage accumulation occurs due to defects production, their motion and interaction with each other and other defects preexisting or have been built up via the interaction

Any interaction with mobile defects, structure and life time of immobile defects proceed with certain rates. The Rate Theory is a tool specially developed for calculations of the rates (kinetics).

Any Radiation Damage Model/Theory, existing or may be developed, is and will be based on Rate Theory!

Radiation Damage Accumulation and Radiation Damage Theory

Depending on how rate theory (Transition State Theory, Chemical Reaction Rate Theory) is used to describe the process several techniques were suggested to resolve these problems:

- Mean field approximation (MFA) - continuum approach which is not limited in space and time however has strong limitations in spatial correlations and fluctuations.
- Kinetic Monte Carlo (KMC) methods - can consider spatial correlations and fluctuations but have strong computational limitations for space and time scales.

Rate Theory and Mean Field Approximation

Theory of Reaction Rates based on statistical thermodynamics.

Also known as The Transition State Theory or Chemical Reaction Rate Theory,

it was developed by M. Polanyi and particularly H. Eyring following earlier work of R. Tolman in 1927 and H. Pelzer and the Hungarian physicist Eugene Paul Wigner in 1932.

H. A. Kramers, 1940, Physica (Utrecht) 7, 284

P. Hanggi, P. Talkner, M. Borkovec, Reaction-rate theory: fifty years after Kramers, Reviews of Modern Physics, Vol. 62, No.2, April 1990.

The problem of escape from metastable states is ubiquitous in almost all scientific areas. Reaction-rate theory has received major contributions from fields as diverse as chemical kinetics, the theory of diffusion in solids, homogeneous nucleation, and electrical transport theory, to name but a few.

The main idea of MFA is to replace all interactions in a many-body system to any one body with an average or effective interaction. This reduces any multi-body problem into an effective one-body problem.

Point is how to describe the average or effective interaction

Microstructure evolution: mean field approach

A general diffusion equation in the mean field approximation for a single absorber (sink) embedded into loss media:

$$\frac{dC_v(r,t)}{dt} = D_v \Delta C_v(r,t) + (G_v(r,t) + G_v^T) - \mu_R D_i C_i(r,t) C_v(r,t) - D_v C_v(r,t) k_v^2,$$

$$\frac{dC_i(r,t)}{dt} = D_i \Delta C_i(r,t) + G_i(r,t) - \mu_R D_i C_i(r,t) C_v(r,t) - D_i C_i(r,t) k_i^2.$$

Here $k_{v,i}^2$ are the sink strengths of the loss media for vacancies and interstitials.

Dimensionality of k^2 is m^{-2} (k^{-1} - the mean 3-D free path)

Sink strength can be obtained by considering a separate problem of diffusion for each particular type of absorber.

Microstructure evolution example: 3-D diffusion and spherical sink

Consider a stationary 3-D diffusion problem of defects near spherical cavity of radius R (where void radius can be estimated from simple geometrical approach $R = (3x\Omega/4)^{1/3}$, x is the number of vacancies in the void):

$$G - k^2 D (C - C^e) - \nabla J = 0 \equiv G - k^2 D (C - C^e) - D \Delta C = 0,$$

here C^e is the thermal-equilibrium concentration (thermal evaporation of vacancies) and $J = -D \nabla C$ the flux of mobile defects, D the defect diffusion coefficient.

For the spherical case Laplacian has the form:

$$\Delta C = \frac{1}{r^2} \frac{\partial}{\partial r} \left(r^2 \frac{\partial C}{\partial r} \right) + \frac{\partial}{\partial \theta} \frac{1}{r^2 \sin \theta} \left(\sin \theta \frac{\partial C}{\partial \theta} \right) + \frac{1}{r^2 \sin^2 \theta} \frac{\partial^2 C}{\partial \varphi^2},$$

The boundary conditions for the defect concentration, C , at the void surface and infinity are:

$$C(R) = C^e, \quad C^\infty = C^e + \frac{G}{k^2 D}.$$

Microstructure evolution : 3-D diffusion and spherical sink

Here all other sinks in the system: voids, dislocations, etc. are considered in the mean-field approximation as the total sink strength k^2 . The procedure is thus self-consistent and the solution is:

$$C(r) = C^e + (C^\infty - C^{eq}) \left\{ 1 - \frac{R}{r} \exp[-k(r - R)] \right\},$$

The defect flux, I , through the void surface $S=4\pi R^2$ is

$$I = -SD\nabla C(r = R),$$

where the sink strength of the void considered for vacancies and interstitials:

$$I_v = D_v (C_v^\infty - C_v^{eq}) 4\pi R (1 + k_v R) \quad \Rightarrow \quad (k_{void}^2(R))_v = 4\pi R (1 + k_v R),$$

$$I_i = D_i (C_i^\infty - C_i^{eq}) 4\pi R (1 + k_i R), \quad \Rightarrow \quad (k_{void}^2(R))_i = 4\pi R (1 + k_i R),$$

where k_v^2, k_i^2 are media sink strengths for vacancies and SIAs

The total sink strength of all voids in the system can be obtained by integration over void size distribution function, $f(R)$:

Microstructure evolution : 3-D diffusion and spherical sink

$$\left(k_{void}^2\right)_v = \int dR \left(k_{void}^2(R)\right)_v f(R) 4\pi \langle R \rangle N_v \left(1 + k_v \frac{\langle R^2 \rangle}{\langle R \rangle}\right) \approx 4\pi \langle R \rangle N_v$$

$$\left(k_{void}^2\right)_i = \int dR \left(k_{void}^2(R)\right)_i f(R) = 4\pi \langle R \rangle N_v \left(1 + k_i \frac{\langle R^2 \rangle}{\langle R \rangle}\right) \approx 4\pi \langle R \rangle N_v.$$

Here $N_v = \int dR f(R)$ is the void number density, $\langle R \rangle$ is the mean radius and $\langle R^2 \rangle$ is the mean square radius of voids.

Typically, $k_v^2 \sim k_i^2 = k^2 \sim 10^{14} m^{-2}$ i.e. $k^{-1} \sim 100$ nm, which is in fact a mean free pass of a 3-D diffusing defect between sinks.

The void radii are much smaller, typically \sim several nm.

Hence, in the vast majority of realistic cases $k^2 \cong 4\pi \langle R \rangle N_v$ with a high accuracy.

An important conclusion is that void has the same sink strength for both vacancies and interstitials, i.e. void is a neutral sink!

Microstructure evolution : 3-D diffusion and PDs recombination

The above solution:

$$C(r) = C^e + (C^\infty - C^{eq}) \left\{ 1 - \frac{R}{r} \exp[-k(r - R)] \right\},$$

can be used to calculate the rate of recombination reactions between vacancies and interstitials.

Considering interstitials motion in the coordinate system where vacancies are immobile their diffusion coefficient is $(D_i + D_v)$ and taking into account that $D_i \gg D_v$, the total recombination rate between vacancies and SIAs is:

$$R = 4\pi r_{eff} (1 + kr_{eff}) (D_i + D_v) C_i n_v \approx 4\pi r_{eff} (1 + kr_{eff}) D_i C_i n_v = \frac{4\pi r_{eff}}{\Omega} D_i C_i C_v,$$

where $R = r_{eff}$ is the recombination effective capture radius. The recombination constant is then: $\mu_R = 4\pi r_{eff} / \Omega$.

MD calculations show that the recombination zone around a vacancy, i.e. a zone where spontaneous recombination of PDs takes place, consists of 100-300 lattice sites, $\left(\frac{4\pi}{3} r_{eff}^3 = (100 - 300)\Omega \right)$ that is ~2-3 lattice parameters thus r_{eff} is usually about 10^{21} m^{-2} .

Microstructure evolution : 3-D diffusion, spherical voids and PDs recombination

Conclusions:

- Voids are neutral sinks and absorb vacancies and interstitial atoms in equal numbers;
- Recombination of vacancies and interstitials also affect them both equally.

Therefore such a system is not able to accumulate radiation damage!!!

However, radiation damage exists!
The reason is mainly the existence of edge dislocations, a necessary part of a material microstructure!

Microstructure evolution: sink strength of dislocations

To estimate dislocation sink strength we should consider the following steady state diffusion equations:

$$0 = G - D_v \Delta C_v(r, t) - D_v C_v(r, t) k^2,$$

$$0 = G - D_i \Delta C_i(r, t) - D_i C_i(r, t) k^2,$$

with the Laplacian for defect concentration in cylindrical coordination system:

$$\Delta C = \frac{1}{\rho} \frac{\partial}{\partial \rho} \left(\rho \frac{\partial C}{\partial \rho} \right) + \frac{1}{\rho^2} \left(\frac{\partial^2 C}{\partial \theta^2} \right) + \frac{\partial^2 C}{\partial z^2},$$

For the sake of simplicity an edge dislocation is approximated as a cylinder of a certain radius which is different for vacancies (R_v) and SIAs (R_i) due to the difference in their interactions with dislocation. The boundary conditions for the case are:

$$C_v(r = R_v) = 0, \quad C_i(r = R_i) = 0,$$

$$C_v(r \rightarrow \infty) = \frac{G}{D_v k^2}, \quad C_i(r \rightarrow \infty) = \frac{G}{D_i k^2}.$$

Microstructure evolution: sink strength of dislocations

The solution is:

$$C_v(r) = \frac{G}{D_v k^2} \left[1 - \frac{K_0(kr)}{K_0(kR_v)} \right],$$

$$C_i(r \rightarrow \infty) = \frac{G}{D_i k^2} \left[1 - \frac{K_0(kr)}{K_0(kR_i)} \right].$$

where $K_0(x)$ is the modified zero-order Bessel function.

With the above boundary conditions the dislocation sink strength for vacancies and interstitials are:

$$\left(k_d^2\right)_v = \rho Z_v, \quad Z_v = \frac{2\pi}{\ln\left(\frac{1}{kR_v}\right)}, \quad \left(k_d^2\right)_i = \rho Z_i, \quad Z_i = \frac{2\pi}{\ln\left(\frac{1}{kR_i}\right)}.$$

where ρ is the dislocation density. $R_v < R_i \implies Z_v < Z_i$

The “dislocation bias” is then defined as: $p_d = (Z_i - Z_v) / Z_v$ (~ a few %)

Microstructure evolution: Standard Rate Theory (SRT)

Consider the case of Frenkel pairs generation and 3-D diffusion of point defects. For this case the total sink strength in the system is a sum of strengths of all sinks i.e. dislocations and voids. Equations for defect balance and expressions for sink strength are:

$$G = D_v C_v \left(k_{tot}^2 \right)_v, \quad G = D_i C_i \left(k_{tot}^2 \right)_i,$$
$$\left(k_{tot}^2 \right)_v = k_{void}^2 + Z_v \rho, \quad \left(k_{tot}^2 \right)_i = k_{void}^2 + Z_i \rho.$$

Swelling rate, i.e. rate of accumulation of vacancies in voids due to different flow of vacancies and interstitials to them:

$$\frac{dS}{d\phi} = 4\pi \langle R \rangle N_v (D_v C_v - D_i C_i),$$

where flux $\phi = Gt$ is irradiation dose, i.e. total number of defects produces by irradiation during time t .

Using above balance equations the swelling rate is estimated as:

$$\frac{dS}{d\phi} = P_d \frac{4\pi \langle R \rangle N_v \rho}{(4\pi \langle R \rangle N_v + \rho)^2},$$

where $S = \frac{4\pi}{3} N_v \langle R \rangle^3$ is the total volume of voids

The maximum of swelling rate is when defect fluxes are distributed equally between the both sinks, i.e. when $4\pi \langle R \rangle N_v = \rho$

$$\left(\frac{dS}{d\phi} \right)_{\max} = \frac{P_d}{4}$$

For typical swelling rates observed experimentally, ~1% per dpa, the dislocation bias is $\sim 4 \times 10^{-2}$. That means dislocations absorb at most 4% more interstitials than vacancies.

Dislocation bias is the basic mechanism of the Standard Rate Theory, It was predicted by Foreman et al. at 1959, i.e. well before swelling was observed in vessel steels by Cawthorne and Fulton at 1966.

Since that the SRT has been used in majority of theoretical models for radiation damage

SRT is a useful and simple tool as introduction to Radiation Damage Theory and can be used for simple estimations. In the case of electron ~ 1 MeV irradiation (Frenkel pairs production) SRT is correct if effects related to the surface and beam size treated properly

Current state and future of Radiation Damage Theory

Practically important damage is produced by high-energy neutrons and ions when primary damage occurs in displacement cascades (see lectures by R.Stoller and R.Averbak).

Main lessons learned from MD modeling of high-energy cascades:

- An intensive intra-cascade clustering is a specific effect in high energy cascades.
- Interstitial clusters are mobile, thermally and kinetically stable and migrate one-dimensionally. Therefore the reaction kinetics governs by a combination 3-D (vacancies and SIAs) and 1-D (SIA clusters) diffusion.

There is no simple balance between the rate of production of single 3-D diffusing vacancies and SIAs, which is in the very heart of SRT basis

New theory have to be developed to account the above features

Such a complicated kinetics is accounted in the Production Bias Model (PBM) develop in the last decade of 20 century:

- **Woo and Singh, 1992, Production bias due to clustering of point defects in irradiation-induced cascades.**
- **Trinkaas, Singh and Foreman, 1992 Glide of interstitial loops produced under cascade damage conditions: Possible effects on void formation.**
- **Singh, Golubov, Trinkaas, Serra, Osetsky and Barashev 1997, Aspects of microstructure evolution under cascade damage conditions.**
- **Golubov, Singh and Trinkaas 2000, Defect accumulation in fcc and bcc metals and alloys under cascade damage conditions-towards a generalization of the production bias model.**
- **Trinkaas, Singh and Golubov, 2000, Progress in modeling the microstructure evolution in metals under cascade damage conditions.**

PBM as it has been formulated is limited for application for real materials and large doses. A reason: the Mean Field approximation is not applicable because 1-D reaction kinetics leads to spatial correlations between defects: voids, dislocations, secondary precipitates and so on. Details can be found:

- Barashev and Golubov, 2009, Unlimited damage accumulation in metallic materials under cascade-damage conditions.
- Barashev and Golubov, 2009, Radiation damage theory: Past, present and future.
- Barashev and Golubov, 2010, On the onset of void ordering in metals under neutron or heavy-ion irradiation.

There are some other issues related to the SIA cluster properties which have to be resolved to complete the PBM. This work is now in progress.

Kinetic Monte Carlo modeling

The kinetic Monte Carlo (KMC) method is a Monte Carlo method computer simulation intended to simulate the time evolution of processes that occur with a given known rate.

The KMC method can be subdivided by how the objects are moving or reactions occurring. At least the following subdivisions are used:

- Lattice KMC (LKMC) signifies KMC carried out on an atomic lattice.

Often this variety is also called atomistic KMC, (AKMC). A typical example is simulation of vacancy diffusion in alloys, where a vacancy is allowed to jump around the lattice with rates that depend on the local elemental composition

- Object KMC (OKMC) means KMC carried out for defects or impurities, which are jumping either in random or lattice-specific directions. Only the positions of the jumping objects are included in the simulation, not those of the 'background' lattice atoms. The basic KMC step is one object jump.

- Event KMC (EKMC) or First-passage KMC (FPKMC) signifies an OKMC variety where the following reaction between objects (e.g. clustering of two impurities or vacancy-interstitial annihilation) is chosen with the KMC algorithm, taking the object positions into account, and this event is then immediately carried out (Dalla Torre 2005, Ooppelstrup 2006).

Kinetic Monte Carlo modeling

The first publications described the basic features of the KMC method: Young and Elcock (1966) and Young (1966). The residence-time algorithm was also published at about the same time by Cox (1965).

Independently Bortz, Kalos and Lebowitz (Bortz 1975) developed a KMC algorithm for simulating the Ising model, which they called the *n-fold way*. The basics of their algorithm is the same as that of (Young 1966), but they do provide much greater detail on the method.

The following year Dan Gillespie published what is now known as the Gillespie algorithm to describe chemical reactions (Gillespie 1976). The algorithm is similar and the time advancement scheme essentially the same as in KMC.

A good introduction is given by Art Voter (Introduction to the Kinetic Monte Carlo Method, Proceedings of the NATO Advanced Study Institute on Radiation Effects in Solids, held in Erice, Sicily, Italy, 17-29 July 2004, Series: NATO Science Series II: Mathematics, Physics and Chemistry, Vol. 235

It is important to understand that all the reactions and their rates are inputs to the KMC algorithm, the method itself cannot predict them. They are usually taken either from lower scale modeling (*ab initio*, MD, etc), estimated from basic theory or, in some cases, from experiments.

Rate Theory and KMC: comparison in calculating of damage accumulation

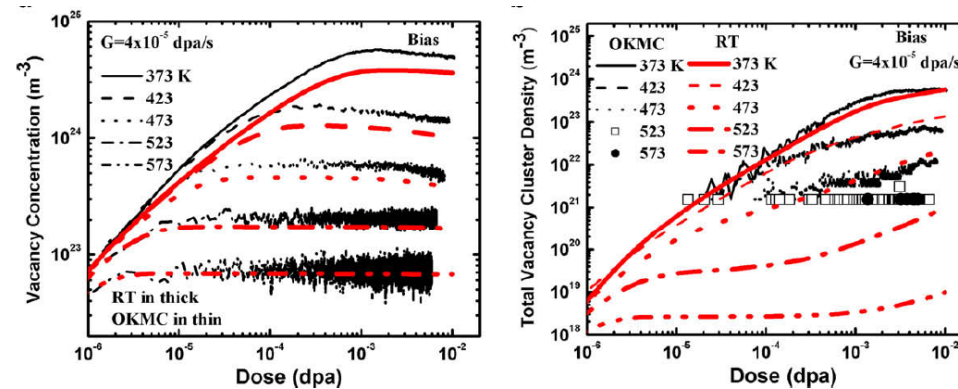
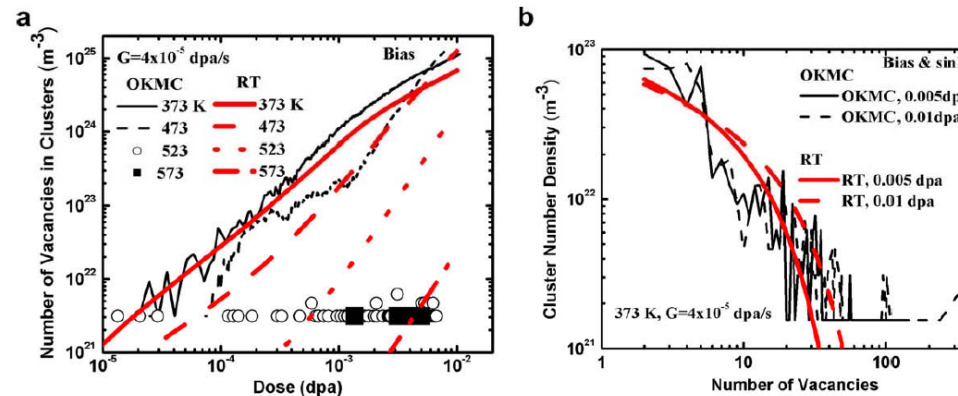


Fig. 8. Influence of irradiation temperature on MFRT and OKMC predictions of (a) vacancy concentration and (b) vacancy cluster density.



- **KMC: Low temperatures, high production rates, low doses. Accounts: spatial correlations, which has not yet been explored**
- **MFRT- no limits with temperature, production rate, doses. Very limited spatial correlations**

RD Theory and Modeling

What is common and what is different?

Common:

- defect properties and interaction
- damage accumulation for KMC and RT

Difference:

- scale, spatial correlations

<i>Ab-initio</i>	$\sim 10^3$ atoms
MD	$10^7 - 10^9$
Lattice KMC	$10^8 (0.1\mu\text{m}) - 10^{11}(1\mu\text{m})$
-----?	
-----?	
Rate theory	10^{24}